ELSEVIER

Journal of Photochemistry and Photobiology
A: Chemistry 86 (1995) 33–71

Journal of
PHOTOCHEMISTRY
AND
PHOTOBIOLOGY
A:CHEMISTRY

Photolysis of tetramethylsilane near the absorption onset: mechanism and photophysics

M. Ahmed [1], P. Potzinger, H.Gg. Wagner

Max Planck Institut für Strömungsforschung, Bunsenstraße 10, 37073 Göttingen, Germany

Received 10 June 1994; accepted 6 September 1994

Abstract

The excitation of tetramethylsilane (Me_4Si) into its lowest excited Rydberg state is followed by two main decomposition channels: a simple Si–C bond breaking process with a quantum yield of $\Phi = 0.45 \pm 0.05$ and a methane elimination process with the concomitant formation of dimethylsilaethylene ($\Phi = 0.17 \pm 0.04$). Other very minor primary processes occur, with quantum yields of the order of $\Phi \leqslant 5 \times 10^{-3}$, but their nature could not be identified with certainty. The reactions leading to the stable products are dominated by radical–radical processes and by radical addition reactions to Me_2SiCH_2. The addition reaction to the Si=C double bond occurs preferentially at the Si site. Satisfactory material balance was obtained indicating that the products were mostly recovered. A number of relative rate constants were determined. Reactions in the presence of NO, MeOH, GeH_4 and SF_6 were also studied. An explanation of the photophysics by a three-state model was attempted. From the experiments, it was concluded that the two decomposition channels occur from different electronic states. The lack of dependence of the CH_4 quantum yield on the experimental parameters (liquid or gaseous phase, etc.) suggests a decomposition from a strongly predissociating state, which is identified with the lowest excited singlet state, while the Si–C bond breaking process is thought to occur from the triplet state. Molecules which reach the ground state live sufficiently long so that deactivation competes successfully with decomposition.

Keywords: Photolysis; Tetramethylsilane; Absorption

1. Introduction

Three investigations of the photolysis of tetramethylsilane (Me_4Si) have been reported [1–3]. In Refs. [1] and [2], 147 nm radiation was used, while in Ref. [3], light with a wavelength close to the absorption onset (170–180 nm) was employed. Gammie et al. [1] attempted to unravel the primary decomposition channels by end product analysis, scavenger experiments and isotopic labelling. The following primary decomposition processes and quantum yields were postulated

$$Me_4Si + h\nu \longrightarrow CH_3 + Me_3Si \qquad \Phi = 0.43$$
$$Me_4Si + h\nu \longrightarrow 2CH_3 + Me_2Si \qquad \Phi = 0.24$$
$$Me_4Si + h\nu \longrightarrow CH_4 + Me_2SiCH_2 \qquad \Phi = 0.17$$
$$Me_4Si + h\nu \longrightarrow H_2 + Me_3SiCH \qquad \Phi = 0.02$$
$$Me_4Si + h\nu \longrightarrow CH_2 + Me_3SiH \qquad \Phi = 0.04$$
$$Me_4Si + h\nu \longrightarrow CH_3 + H + Me_2SiCH_2 \qquad \Phi = 0.10$$

The work in Ref. [1] was hampered by an unsatisfactory material balance, familiar to all who work in the field of silicon chemistry. This can be seen quite clearly if we compare the material balances calculated from the quantum yields of the retrieved products, $\Phi(Si) = 0.54$, $\Phi(C) = 2.80$ and $\Phi(H) = 9.04$, with those from the mechanism given, $\Phi(Si) = 1.39$, $\Phi(C) = 5.56$ and $\Phi(H) = 16.68$. This large difference casts doubt not only on the quantum yields given for the primary processes, which were obtained under the constraint $\Sigma\Phi_i = 1.0$, but also on the nature of the proposed decomposition channels.

The work of Tokach and Koob [2] was less detailed with respect to the primary processes and concentrated mainly on the reactivity of the trimethylsilyl radical and on the yield of silaethylene formation. Only four products were observed: $\Phi(CH_4) = 0.36$, $\Phi(C_2H_6) = 0.53$, $\Phi(Me_3SiH) = 0.12$ and $\Phi(Me_6Si_2) = 0.12$. With the

[1] Present address: Department of Chemistry, University of Manchester, Manchester, UK.

SSDI 1010-6030(94)03953-4

exception of $\Phi(C_2H_6)$, which is higher by a factor of 1.5, the quantum yields are in good agreement with those given in Ref. [1]. Again the material balance points to very poor product retrieval. The main point made in the paper was the very high reactivity of the trimethylsilyl radicals. It was found that Me_3Si reacts more than ten times faster than CH_3 in abstracting a D atom from such molecules as CD_4, D_2S and CD_3OH. This was later explained [3] to be due to hot radical formation during 147 nm photolysis. Many steps in the mechanism proposed by Gammie et al. [1] also imply the participation of hot radicals.

The investigation reported in Ref. [3] is distinguished from the other two in that irradiation at the long-wavelength end of the absorption region was conducted in the gaseous as well as in the liquid phase and the products were also studied as a function of temperature. Great effort was made to obtain a product analysis which was as quantitative as possible. Three primary processes were found

$$Me_4Si + h\nu \longrightarrow CH_3 + Me_3Si \qquad \Phi = 0.55 \pm 0.17$$

$$Me_4Si + h\nu \longrightarrow CH_4 + Me_2SiCH_2 \qquad \Phi = 0.22 \pm 0.07$$

$$Me_4Si + h\nu \longrightarrow H + Me_3SiCH_2 \qquad \Phi \geqslant 0.01$$

For the first time, the reaction pathways of Me_2SiCH_2 could be followed by the observed product pattern. Me_2SiCH_2 was found to undergo dimerization as well as radical addition reactions. In addition, the radicals undergo all conceivable combination processes. More quantitative information, especially on radical disproportionation reactions, could not be obtained because of the unfortunate choice of photolysis source, an iodine lamp. The most intense emission line, $\lambda = 206$ nm, is not absorbed by Me_4Si but is very strongly absorbed by all products with an Si–Si bond, which leads to strong secondary photolysis. Photolyses at elevated temperatures showed quite clearly that the product spectrum is governed by hydrogen abstraction from Me_4Si by the radicals present. Contrary to the findings in Ref. [2], CH_3 radicals were more reactive than Me_3Si radicals, at least with respect to Me_4Si as hydrogen donor.

The photolysis of Me_4Si was taken up again as part of a project to study the reaction pathways of silicon-centred radicals. The results in Ref. [3] suggest that the long-wavelength photolysis of Me_4Si is a rather clean source of a 1 : 1 mixture of CH_3 and Me_3Si radicals and Me_2SiCH_2. Before embarking on a study of the time dependence of these species, it was thought advisable to obtain a knowledge of the whole reaction mechanism which is as quantitative as possible. Therefore a quantitative product analysis, quantum yield determination and study of the effects of different additives at the ArF laser line and two wavelengths close to it were performed providing not only a knowledge of the reaction mechanism but also semiquantitative information on radical–radical reactions and radical addition to the Si=C double bond.

2. Experimental details

Gas handling was performed on a conventional vacuum line. Gas pressures were measured by capacitance manometers (MKS 122, 10 mbar, 1000 mbar). The photolysis lamp–photolysis cell unit was integrated into the vacuum line and was also attached to a vacuum UV monochromator (Minuteman 302VM). The dispersed radiation was monitored by a solar blind photomultiplier. This arrangement allowed the lamp intensity to be set to a reproducible level and line impurities to be checked.

The photolysis lamp and reaction cell for 175 nm radiation were interfaced by an MgF_2 window. The cylindrical reaction cell had a volume of 65 cm^3 and a diameter of 2.5 cm. The microwave powered lamp (EMS Microtron 200) had a continuous flow of 1% N_2 in helium. The flow and pressure were regulated by metering valves. A molecular sieve filter prevented the back flow of oil vapour from the roughing pump. The quantum flux of the lamp was about 3×10^{14} photons s^{-1}; the exact value was determined before and after each set of experiments by actinometric methods.

At 185 nm, a low-pressure mercury arc (Gräntzel Typ 5) was used. The thermostatically controlled lamp was purged by a continuous flow of N_2. The quantum flux of the lamp was 2×10^{16} photons s^{-1}. The cylindrical quartz cell had a volume of 185 cm^3 and an optical path length of 10 cm.

An excimer laser (Lambda Physics) was used for 193 nm photolysis. The cylindrical quartz cell had a volume of 204 cm^3 and an optical path length of 50 cm. The photon flux was 3.6×10^{15} photons per pulse and the repetition rate was 1.25 Hz.

All substances were of commercial origin and of the highest purity grade available. Additionally, tetramethylsilane was purified by preparative gas chromatography before use. All experiments were performed at room temperature (296 ± 2 K).

Photon fluxes into the photolysis cell were determined by actinometry with HBr [4] ($\Phi(H_2) = 1.0$, $\lambda \geqslant 175$ nm) and C_2H_4 [5] ($\Phi(H_2) = 0.4$, $\lambda = 175$ nm). There was excellent agreement between these two actinometers at 175 nm.

End product analyses were performed by mass spectrometry (MAT 311A) and gas chromatography (HP 5890). The overall amount of non-condensable products was determined by pressure measurements. The condensable products were separated using an OV1 fused

silica capillary column (50 m, $\phi_i = 0.32$ mm, 1.5 μm). The inlet system consisted of a multivalve arrangement which could be evacuated. The sample was expanded from a thermostatically controlled bulb into the thermostatically controlled sample loop. The pressure in the sample loop was measured by a capacitance manometer (Valyndine). For quantitative evaluation of the chromatograms an internal standard (propane) was used. All samples were analysed at least twice. Response factors were determined for a number of Si–C–H compounds. As can be seen from Fig. 1, there is a good linear relationship between the sensitivity of a compound and the number of carbon atoms it contains. All products observed have been identified in Ref. [3].

3. Results

The absorption spectrum of Me_4Si over an extended wavelength region has been reported by several groups [6,7]. The first structureless absorption band reaches from the onset to about 155 nm. The extinction coefficient as a function of wavelength near the absorption onset is given in Fig. 2.

3.1. Photolysis at 193 nm

When the full laser beam was employed for sample irradiation, large amounts of non-condensable products with only trace amounts of silicon-containing products were detected. This is due to the secondary photolysis of products, especially those with an Si–Si chromophore which exhibit very large extinction coefficients ($\epsilon \approx 10^4$ M^{-1} cm^{-1}) and which, even at very small concentrations,

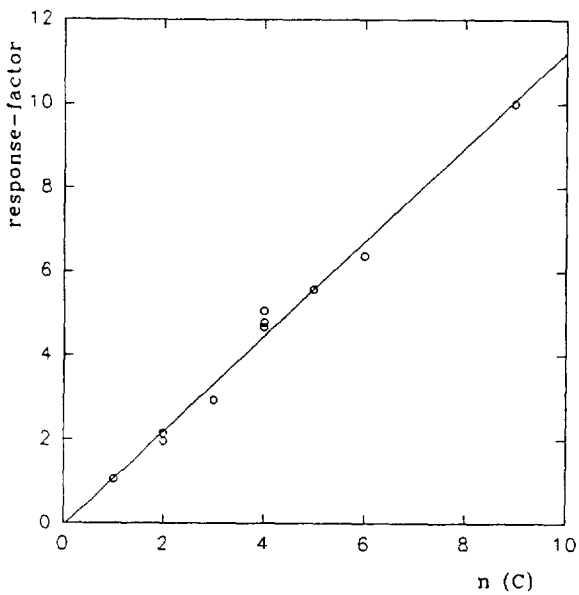

Fig. 1. Gas chromatographic response of various silicon compounds vs. the number of carbon atoms they contain.

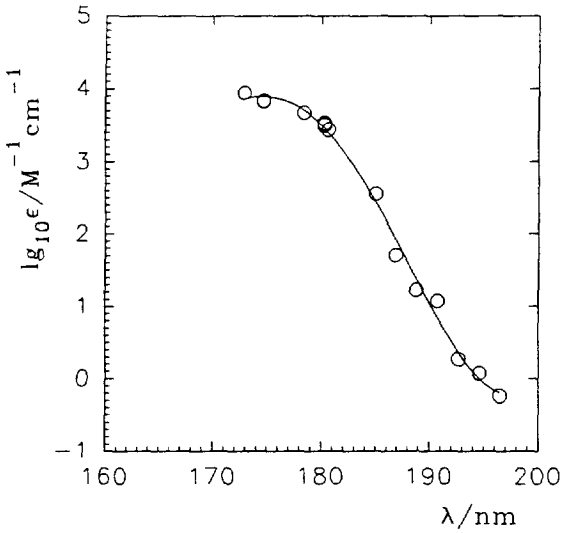

Fig. 2. Extinction coefficient of Me_4Si as a function of wavelength near the absorption onset.

compete successfully with Me_4Si ($\epsilon = 1.9 \pm 0.5$ M^{-1} cm^{-1}) for 193 nm quanta. Polymer formation at the entrance window is an additional complicating factor. Reducing the cross-section of the laser beam to 0.05 cm^2, which allows the photosensitive products to hide in the non-illuminated volume of the photolysis cell, yields a product spectrum which is, at least qualitatively, in agreement with that found in Ref. [3]. However, this arrangement was not sufficient to prevent secondary photolysis completely as can be seen from Fig. 3. The quantum yields of all the products decrease with an increasing number of absorbed photons. A second degree polynomial was fitted to the experimental points, shown as a curve in Fig. 3; the constant term is quoted in Table 1. While the quantum yields of the transparent products, CH_4 and C_2H_6, extrapolate to the values found on photolysis at 185 nm and 175 nm, only greatly reduced values are obtained for di- and tri-silanes. A few compounds, such as Me_3SiH, extrapolate to a higher value, indicating that these products are also formed by secondary photolysis.

Increasing the pressure affects transparent and light-sensitive products quite differently (Fig. 4). The quantum yields of the transparent products decrease with increasing pressure, while compounds containing an Si–Si group show increases in their quantum yields.

3.2. Photolysis at 185 nm

In Fig. 5, the number of molecules formed is plotted vs. the number of photons absorbed. The plots show considerable curvature, indicating that secondary photolysis is still taking place. The experimental points were fitted by a function $n = aq + bq^2$ (n is the number of molecules, q is the number of photons) shown as a line. The coefficient a is taken to be equal to the

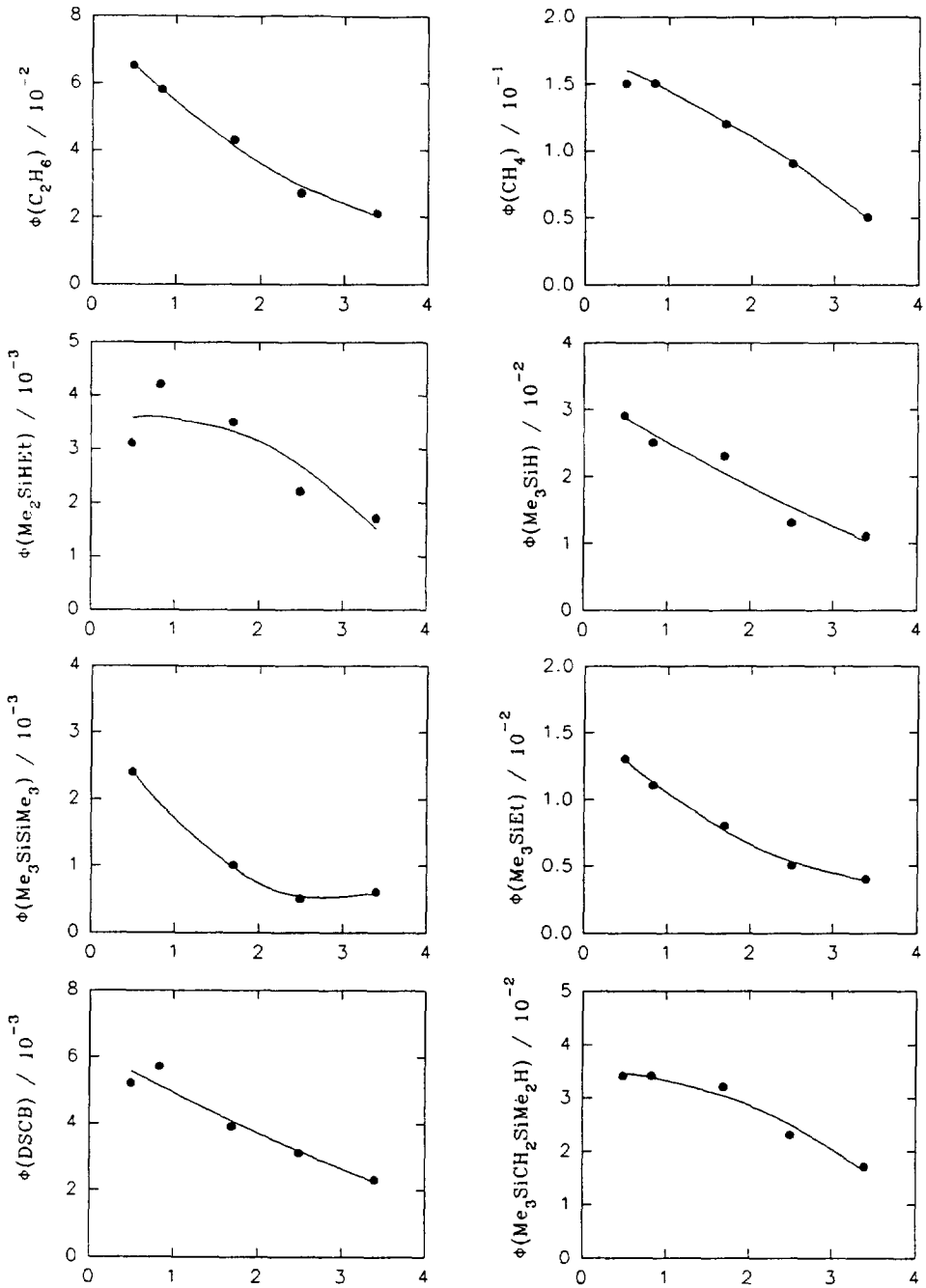

Fig. 3. *(continued)*

quantum yield and this value is listed in Table 1. The quantum yields of those products prone to secondary photolysis increase substantially from their values at 193 nm caused by a greatly increased value of the extinction coefficient of Me_4Si ($\epsilon(185\ nm) = 368 \pm 24\ M^{-1}\ cm^{-1}$). Under the conditions of Fig. 5, no H_2 was detected, but at a higher pressure (200 mbar) and prolonged irradiation (15 min) a value of $\Phi(H_2) \approx 0.006$ was determined. The determination is approximate and has a high degree of uncertainty. No dependence of the product quantum yields was observed up to 200 mbar.

A number of additives were used in the photolysis to elucidate the mechanism. The addition of NO leads to the disappearance of most of the products with three notable exceptions (Fig. 6). Methane is almost unaffected by the addition of NO, while the quantum yields of Me_3SiEt and Me_3SiH contain a small portion which must be formed by non-radical processes. The non-scavengeable quantum yields, denoted by Φ(product/scavenger), are $\Phi(Me_3SiEt/NO) = 1.7 \times 10^{-3}$ and $\Phi(Me_3SiH/NO) = 2.5 \times 10^{-3}$. These values are listed in Table 1. From the dependence of $\Phi(C_2H_6)$ and $\Phi(Me_6Si_2)$ in Fig. 6, it can be inferred that NO reacts

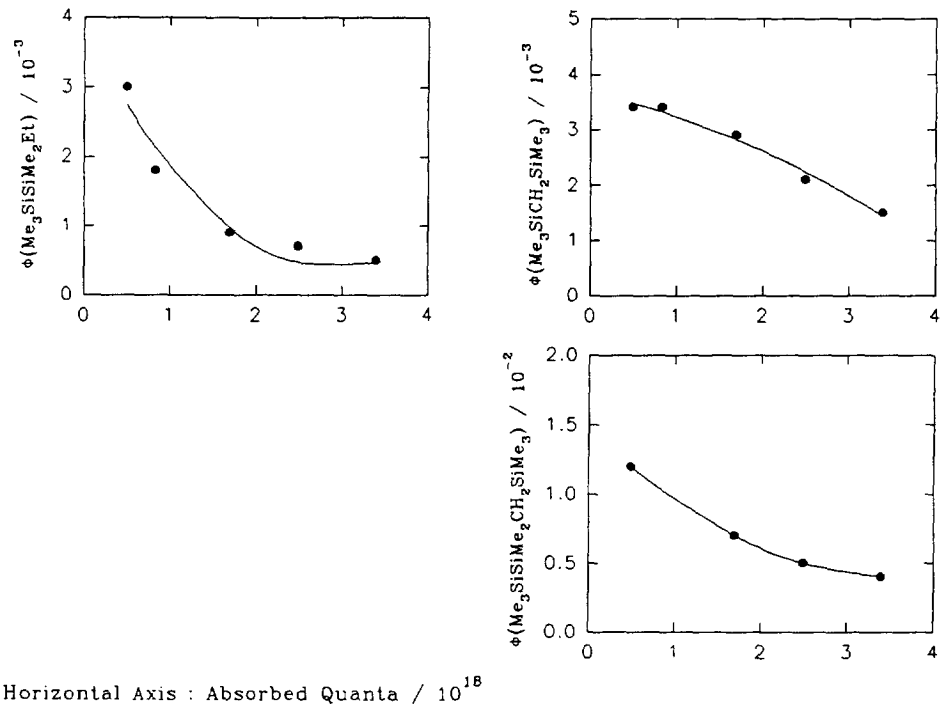

Fig. 3. Dependence of the product quantum yields on the number of absorbed quanta in the 193 nm photolysis of 34 mbar Me_4Si.

Table 1
Experimental and simulated quantum yields

Product	Φ(193 nm)/10^{-2}	Φ(185 nm)/10^{-2}	Φ(175 nm)/10^{-2}	Φ(calc)/10^{-2}
CH_4	16±2	18.6±1.8	18.5±0.8	20
C_2H_6	7.8±0.3	10.5±0.7	10.8±0.3	11
Me_3SiH	3.2±0.4	1.3±0.2	2.2±0.2	1.2
Me_3SiEt	1.6±0.1	1.0±0.1	1.17±0.04	1.2
Me_2HSiEt	0.34±0.10	0.18±0.03	0.40±0.05	0.19
Me_6Si_2	0.33±0.01	5.17±0.31	5.73±0.22	6.1
$Me_2HSiCH_2SiMe_3$	0.35±0.03	0.20±0.04	0.44±0.06	0.21
DSCB	0.62±0.08	2.91±0.23	2.13±0.11	3.3
$Me_3SiCH_2SiMe_3$	0.37±0.02	0.94±0.07	0.95±0.07	0.9
$Me_3SiSiMe_2Et$	0.39±0.05	3.30±0.23	2.75±0.20	3.5
$Me_3SiSiMe_2CH_2SiMe_3$	1.5	3.36±0.42	2.71±0.17	3.8
CH_4/NO		17.0±4.1		
Me_3SiH/NO		0.25	0.25	
Me_3SiEt/NO		0.175	0.24	
Me_3SiEt/MeOH		0.20±0.01	0.43±0.03	
$Me_3SiCH_2SiMe_3$/MeOH		0.14±0.02	0.24±0.02	
C_2H_6/MeOH			12.2±0.4	
Me_6Si_2/MeOH		9±1	9.8±0.2	
Me_3SiOMe/MeOH			18±1	
H_2/MeOH		2.0±0.4		

DSCB, 1,1,3,3-tetramethyl-1,3-disilacyclobutane.

faster with Me_3Si radicals than with Me radicals. Products not shown in Fig. 6 have completely disappeared at the smallest NO concentration applied. Product peaks from the reaction of NO with the radicals present have been recorded but not identified.

MeOH was added to obtain information on the mechanistic pathways of Me_2SiCH_2. Different types of behaviour of the products are discernible from Fig. 7. A group of substances (1,1,3,3-tetramethyl-1,3-disilacyclobutane (DSCB), $Me_3SiSiMe_2Et$ and $Me_3SiSiMe_2CH_2SiMe_3$) disappear completely at very small MeOH concentrations. Me_3SiEt and $Me_3SiCH_2SiMe_3$ disappear rapidly at low MeOH concentration, like the products of the first group; however, the quantum yields do not drop to zero but go through a minimum and then increase linearly. The extrapolated

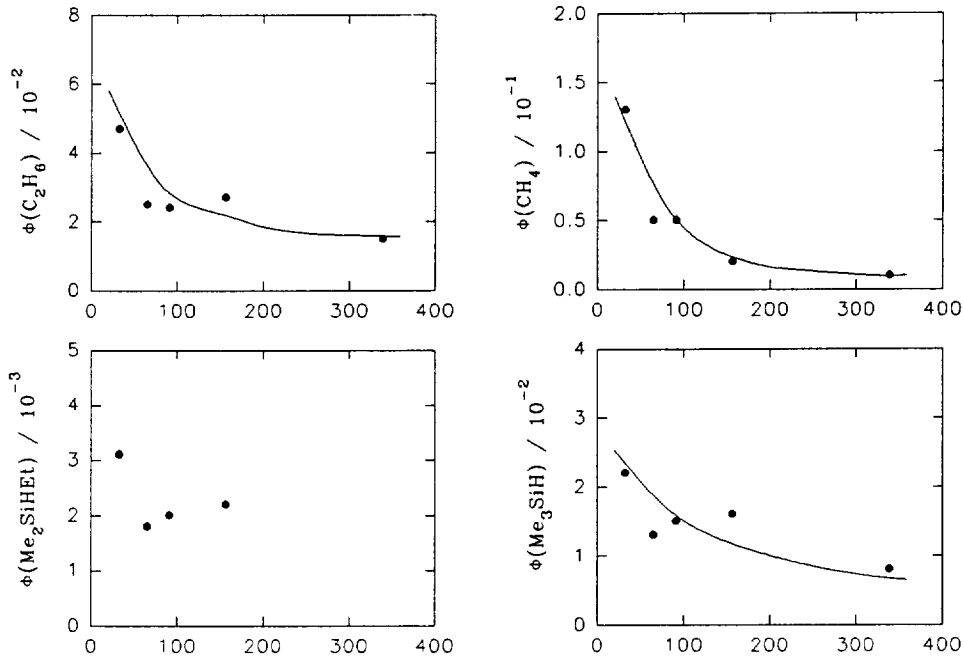

Fig. 4. (*continued*)

linear branch of the curve for Me_3SiEt intersects the ordinate at $\Phi(Me_3SiEt/MeOH) = (2.0 \pm 0.1) \times 10^{-3}$ and for $Me_3SiCH_2SiMe_3$ at $\Phi(Me_3SiCH_2SiMe_3/MeOH) = (1.4 \pm 0.2) \times 10^{-3}$, indicating that this portion of the quantum yield is not scavengeable by MeOH. The Me_6Si_2 quantum yield exhibits a maximum as a function of MeOH concentration. The extrapolation of the linear descending part of the curve cuts the ordinate axis at $\Phi(Me_6Si_2/MeOH) = 0.09 \pm 0.01$. The quantum yield of Me_3SiH increases steadily with increasing MeOH concentration. The well-known product of the reaction of Me_2SiCH_2 with MeOH, Me_3SiOMe, reaches a plateau at rather small MeOH concentrations. The plateau coincides approximately with $\Phi(CH_4)$. Another product, $Me_3SiCH_2SiMe_2OMe$, is only detected at very low MeOH concentration. Rather large amounts of H_2, $\Phi(H_2/MeOH) = 0.020 \pm 0.004$, are found in the presence of MeOH.

GeH_4 was introduced in an attempt to intercept possible hot radicals formed in the primary photochemical processes. However, thermalized Me_3Si radicals produced in the Hg-sensitized photolysis of Me_3SiH react quite effectively with GeH_4 by abstraction [8]. Therefore the quantum yields of the products whose formation involves Me_3Si as a reactant decrease with the addition of germane (Fig. 8). The product of the abstraction process, Me_3SiH, is formed in larger quantities than anticipated from the vanished products. Methyl radicals react much more slowly with GeH_4 than do Me_3Si radicals. The increase in the quantum yield of Me_2EtSiH correlates with the decrease in Me_3SiEt.

Another indicator for the appearance of hot species, SF_6, was introduced into the system, but no significant change in the product spectrum could be detected. Only Me_2EtSiH and $Me_3SiCH_2SiMe_2H$ are suppressed by the addition of SF_6 (Fig. 9). The decrease in the quantum yields of most of the products is probably caused by traces of water, which could not be removed completely from SF_6 by repeated distillation through a P_4O_{10} column (Me_3SiOH and Me_6Si_2O are significant product peaks).

3.3. Photolysis at 175 nm

With the exception of Me_2EtSiH and $Me_3SiCH_2SiMe_2H$, both of which are also formed by secondary processes (Fig. 10), the product yields show a linear dependence on the number of absorbed quanta. The (initial) slopes have been equated to the quantum yields and are compiled in Table 1.

Scavenging experiments were performed with greater resolution than at 185 nm. To show the different dependences of the products on the NO pressure, different scales for the horizontal axes are used in Fig. 11. The overall picture is the same as at 185 nm, i.e. the very fast disappearance of DSCB, $Me_3SiSiMe_2SiMe_3$ and $Me_3SiSiMe_2Et$, the faster scavenging of Me_3Si radicals than of CH_3 radicals and the disclosure of a molecular component in the products Me_3SiEt and Me_3SiH. For Me_3SiH, the quantum yield of the non-scavengeable part, $\Phi(Me_3SiH/NO) = 2.5 \times 10^{-3}$, is the same as at 185 nm, but it is somewhat higher for Me_3SiEt, $\Phi(Me_3SiEt/NO) = 2.4 \times 10^{-3}$. Mechanistic significance is probably contained in the fine structure of

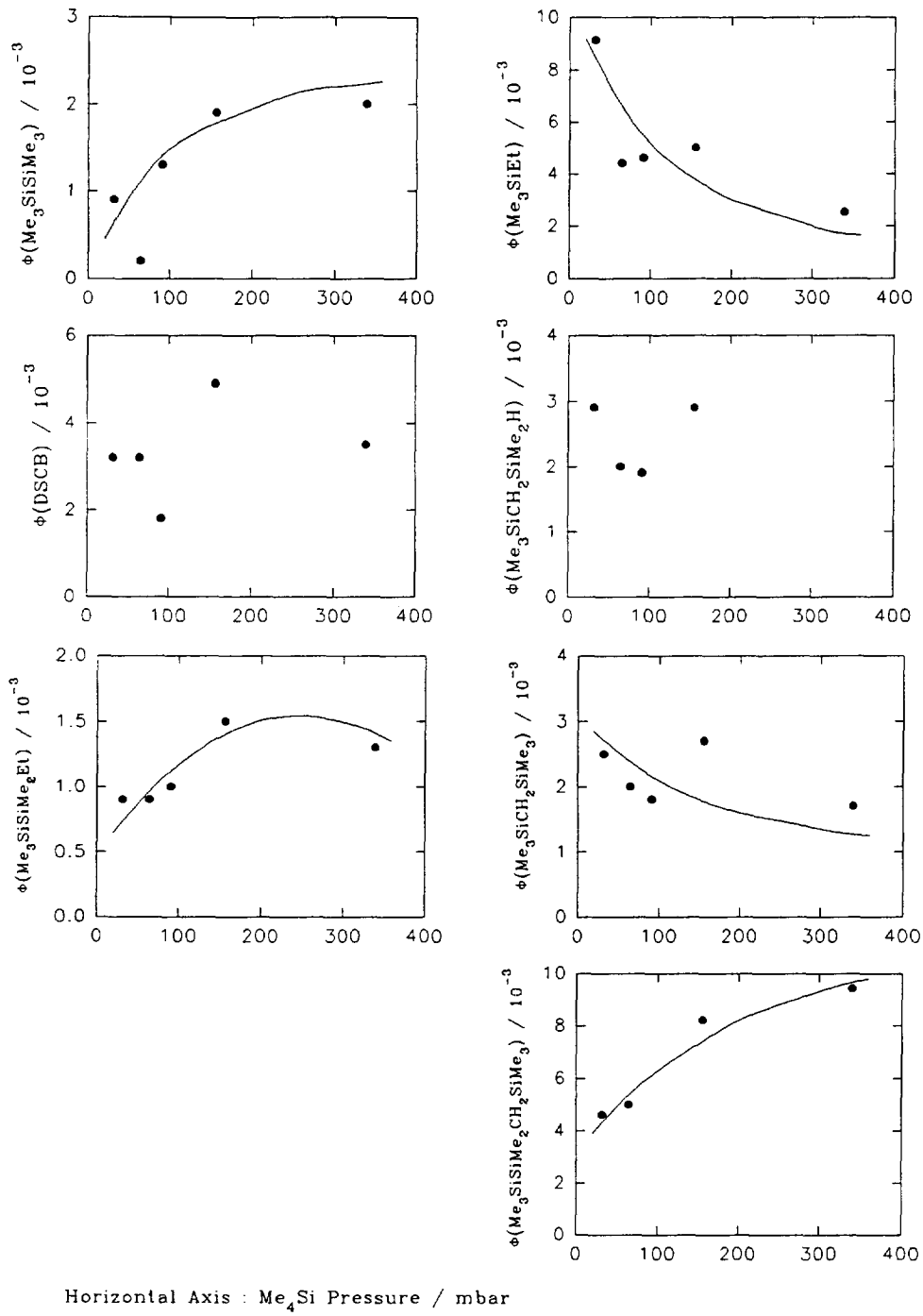

Fig. 4. Dependence of the product quantum yields on the Me_4Si pressure in the 193 nm photolysis of Me_4Si.

the quantum yield vs. [NO] curves of the different products. At low NO concentration, $\Phi(C_2H_6)$ goes through a maximum; the same shape is also observed with Me_3SiH but with a much more pronounced maximum. For Me_3SiEt, it is not clear whether the quantum yield decreases steadily or $\Phi(Me_3SiEt)$ goes through a minimum followed by a maximum. In the case of $Me_3SiCH_2SiMe_3$, two different processes with different time scales appear to occur.

For a number of products, the MeOH experiments at 175 nm give significantly different results from those at 185 nm (Fig. 12). For Me_6Si_2, Me_3SiEt and $Me_3SiCH_2SiMe_3$, the extremes have disappeared and a plateau is observed instead; the plateau quantum yields are given in Table 1. With increasing MeOH concentration, $\Phi(Me_3SiH)$ no longer increases. The two products, Me_2EtSiH and $Me_3SiCH_2SiMe_2H$ are not affected by MeOH as can be seen clearly in Fig. 12.

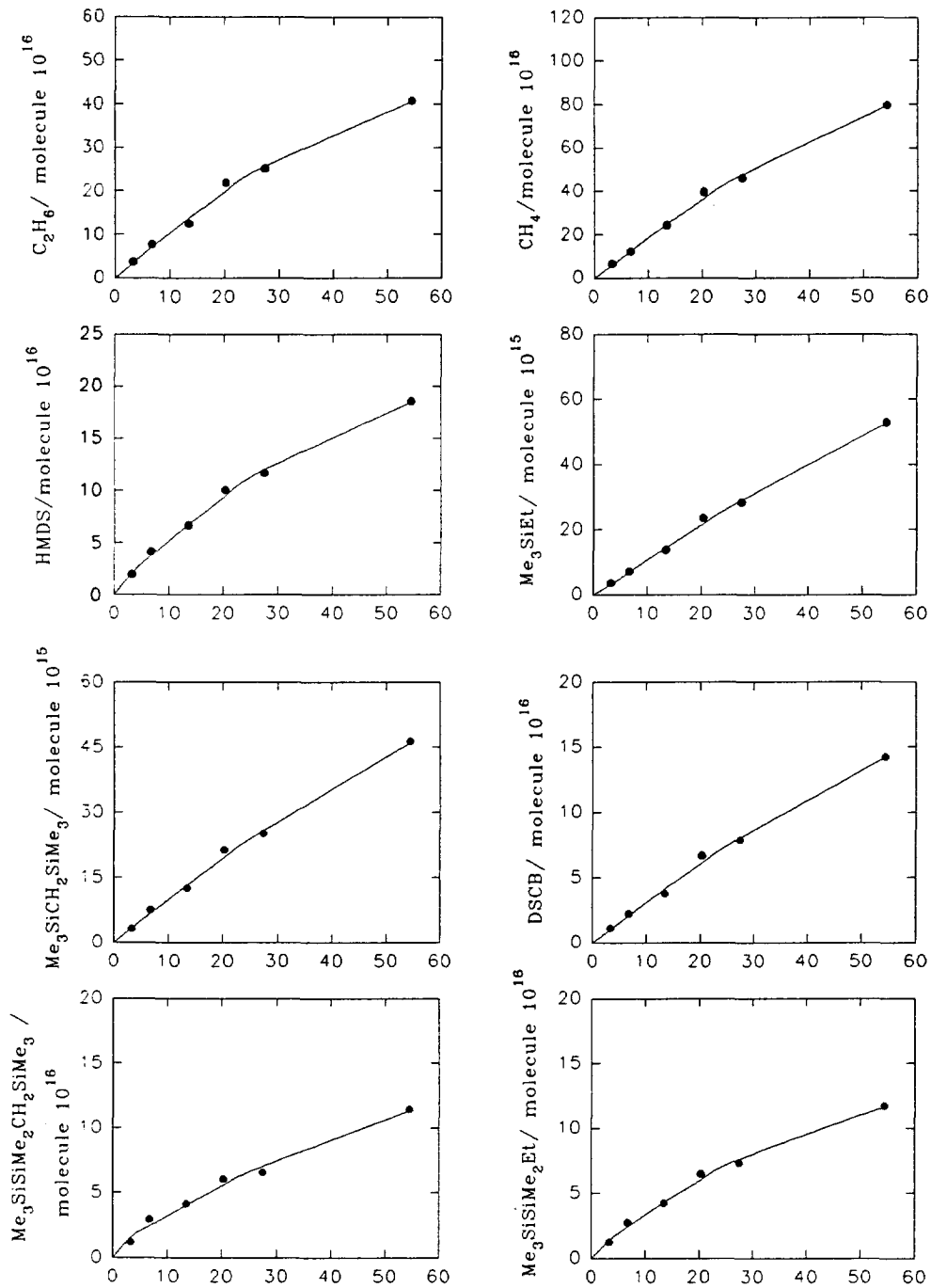

Fig. 5. *(continued)*

A plateau value of $\Phi(Me_3SiOMe/MeOH) = 0.18 \pm 0.01$ is reached by Me_3SiOMe.

The experiments with GeH_4 were hindered by polymer formation and there was an intensity loss during photolysis. To make an evaluation possible, it was assumed that $\Phi(C_2H_6) = 0.1$, independent of GeH_4 concentration. The results resemble those at 185 nm (Fig. 13).

The results obtained in the presence of SF_6 are very similar to those found at 185 nm (Fig. 14).

4. Discussion

The quantum yields of the observed products given in Table 1 show only small changes when the irradiation wavelength is changed from 175 to 185 nm. The large changes observed at 193 nm, especially for di- and trisilanes, are not due to a change in the photochemical behaviour of the Me_4Si molecule, but to secondary photolysis. This can be shown by a model calculation which assumes that the product under consideration

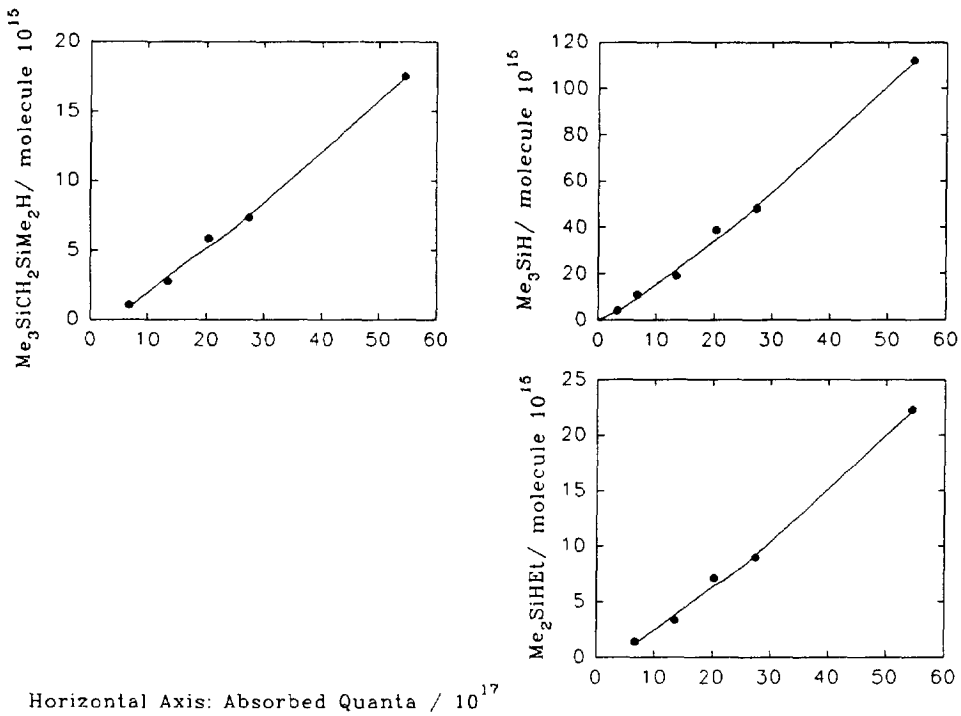

Fig. 5. Dependence of the product yields on the number of absorbed quanta in the 185 nm photolysis of 13.3 mbar Me_4Si. (HMDS = $Me_3SiSiMe_3$.)

is formed with the same quantum yield at 193 and 185 nm, the products distribute uniformly over dark and illuminated volumes of the photolysis cell, the fraction of light absorbed by substance i is given by $(\epsilon_i c_i)/(\Sigma_i \epsilon_i c_i)$ and the product decomposes with a quantum yield of unity. There is good agreement between experiment and calculation (Fig. 15). The decrease in the quantum yield of transparent products, such as CH_4, is due to polymer deposition on the entrance window, which is easily visible. The very different pressure dependences of the quantum yields of transparent and light-sensitive products can be understood as follows. With increasing pressure more light is absorbed near the entrance window leading to an increased polymer deposit on the window. This effect results in a decrease in the quantum yields of all the products. In addition, for the light-sensitive products, an opposing effect is operating which results in a decrease in secondary photolysis; a greater fraction of the light is absorbed by Me_4Si resulting in an effective increase in the non-illuminated volume of the photolysis cell. The second effect prevails over the first. From this study, it is concluded that the product patterns at 193, 185 and 175 nm are essentially the same. This conclusion is important in so far as the results at 193 nm were obtained at a light intensity many orders of magnitude higher than that at the other two wavelengths.

Because all three wavelengths employed in this experiment lie near the edge of the first absorption band, it is assumed that the same excited state is reached in all cases and, to a first approximation, the number, identity and relative importance of the decomposition processes are the same within the wavelength region under investigation. Therefore the results obtained at the different wavelengths will be used collectively to draw inferences on the nature and importance of the different decomposition channels. This necessitates a product retrieval which is as complete as possible. As a first check, the quantum yields of the elements comprising Me_4Si are calculated from the results given in Table 1. The quantum yields, $\Phi(Si) = 0.376 \pm 0.016$, $\Phi(C) = 1.589 \pm 0.051$ and $\Phi(H) = 4.822 \pm 0.153$ at 185 nm and nearly identical values at 175 nm are recovered. Normalizing $\Phi(H)$ to 12.0, we calculate the empirical formula $Si_{0.94 \pm 0.05}C_{3.95 \pm 0.13}H_{12.0}$. Only a slight selective loss of silicon is seen. The fact that $\Phi(-Me_4Si)$ is much smaller than unity will be discussed in Section 4.7.

4.1. The primary decomposition channels

Three mechanistic routes can lead to methane, which is a primary product (Figs. 5 and 10): molecular elimination in the primary decomposition reaction, H atom abstraction by CH_3 radicals and radical–radical disproportionation reactions. The last two routes can be blocked by radical scavengers such as NO. In this case, the methane quantum yield is only slightly, if at all, affected by NO, and so it must be concluded that the predominant part is

$$Me_4Si + h\nu \longrightarrow CH_4 + Me_2SiCH_2 \quad (I)$$

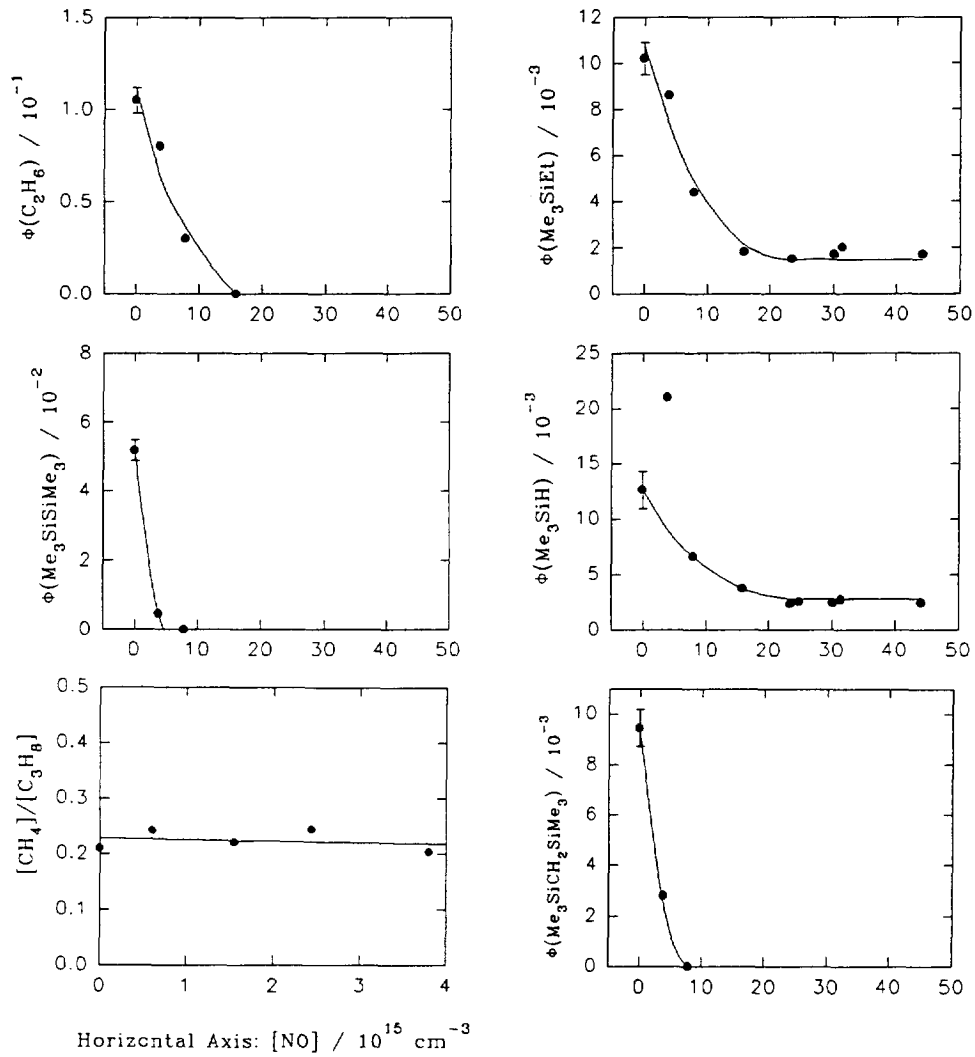

Fig. 6. Dependence of the product quantum yields on NO concentration in the 185 nm photolysis of 13.3 mbar Me_4Si.

Another prominent primary product is ethane. Again molecular and/or radical pathways to its formation are conceivable. Experiment points unambiguously to a radical pathway (Figs. 6 and 11). Methyl radicals can be formed in two ways

$$Me_4Si + h\nu \longrightarrow CH_3 + Me_3Si \quad (II)$$

$$Me_4Si + h\nu \longrightarrow 2CH_3 + Me_2Si \quad (III)$$

Because of energetic considerations, channel (III) is not valid at the longest wavelength applied (193 nm): $\Delta H^{\circ}(III) = 2(146)[9] + 133[10] + 231[11] = 656$ kJ mol^{-1}. A photolysis wavelength shorter than 185 nm is required for reaction (III) to occur. In principle, all the products can be rationalized by the two primary processes (I) and (II). Radical combination can lead to both C_2H_6 and Me_6Si_2. Radical disproportionation can form products with Si–H bonds and dimerization of and radical addition to Me_2SiCH_2 can lead to the products not accounted for by the processes above. If this were true, all the products should be scavengeable by NO and all the products which contain the $-(Me_2SiCH_2)-$ structural unit should be scavengeable by MeOH. This is true to a very large extent, but small unscavengeable amounts of Me_3SiEt and Me_3SiH, by NO, and non-scavengeable amounts of Me_3SiEt and $Me_3SiCH_2SiMe_3$ by MeOH, suggest the presence of other minor primary processes.

That part of Me_3SiEt which cannot be scavenged by NO must be formed by a bimolecular non-radical process. The number of possible processes can be narrowed down by noting that the plateau values of Me_3SiEt and Me_3SiH are nearly identical (here, the much more precise values at 175 nm are relied upon) implying that their formation should therefore be closely related. Two completely different mechanisms may explain their formation: molecular elimination of Me_3SiH with concomitant formation of singlet methylene

$$Me_4Si + h\nu \longrightarrow Me_3SiH + {}^1CH_2 \quad (IVa)$$

followed by $^1CH_2$ insertion into the C–H bond of Me_4Si

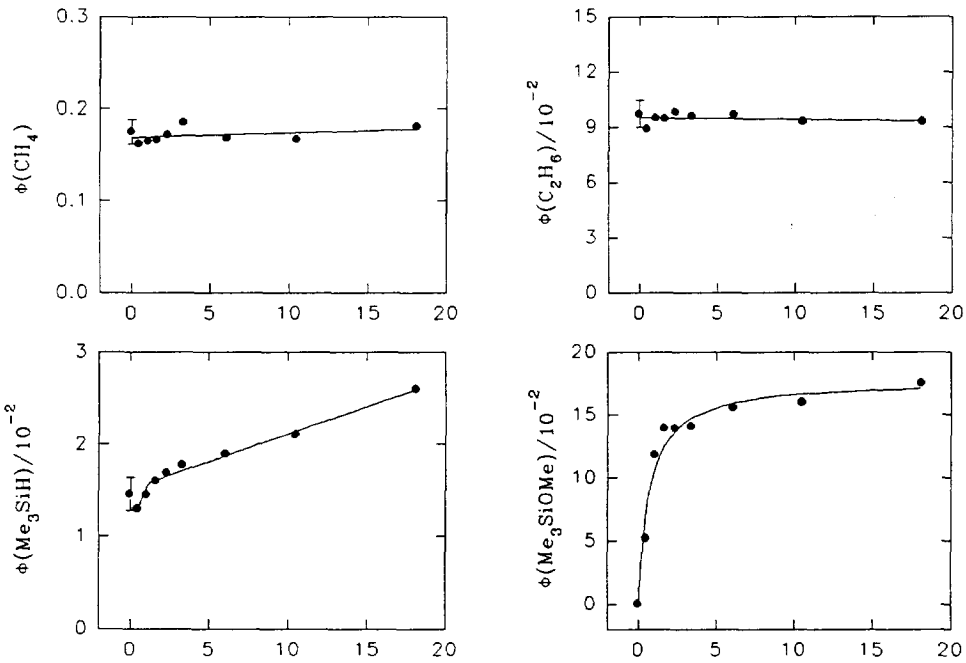

Fig. 7. (*continued*)

$$^1CH_2 + Me_4Si \longrightarrow Me_3SiEt \quad (1)$$

and electronic excitation of Me_4Si leading directly or by internal conversion to a metastable state which is sufficiently long lived to undergo collisions

$$Me_4Si + h\nu \longrightarrow Me_4Si^{**} \quad (IVb)$$

$$Me_4Si^{**} + Me_4Si \longrightarrow Me_3SiH + Me_3SiEt \quad (2)$$

For both suggested channels, objections may be raised. Channel (IVa) is very demanding energetically (ΔH(IVa) = 495 kJ mol^{-1}) and decomposition must take place in the ground state, where it has to compete with other more favourable processes (see Section 4.7). Additionally, deactivation of $^1CH_2$ to the ground state would destroy the 1 : 1 relation between Me_3SiH and Me_3SiEt. In view of our considerations in Section 4.7, the metastable state can only be a highly vibrationally excited ground state and reaction (2) must be characterized as improbable at the very best.

The main formation process of Me_3SiEt is by methyl radical addition to Me_2SiCH_2. This channel should be equally scavengeable either by MeOH or NO. Experiments show, however, that the non-scavengeable fraction is larger in the presence of MeOH than in the presence of NO. Therefore, in addition to processes (1) or (2), another process for Me_3SiEt formation must exist, which must be a pure radical process and must not involve Me_2SiCH_2 as a reactant. For Me_3SiEt, the quantum yield of this new process is $\Phi = 4.3\times10^{-3} - 2.5\times10^{-3} = 1.8\times10^{-3}$. The nature of this new process may be inferred by examining the behaviour of the product $Me_3SiCH_2SiMe_3$ in the presence of MeOH and NO. This product is totally scavenged by NO, but in the presence of MeOH, a small fraction remains whose quantum yield is $\Phi = 2.4\times10^{-3}$. Here, just as in the case of Me_3SiEt, another formation process must exist. The similar behaviour of the two products suggests that the formation processes are related. Both of these products contain the structural unit Me_3SiCH_2; therefore the following two processes are postulated

$$Me_3SiCH_2 + CH_3 \longrightarrow Me_3SiEt \quad (3)$$

$$Me_3SiCH_2 + Me_3Si \longrightarrow Me_3SiCH_2SiMe_3 \quad (4)$$

Because the rate constants and the steady state concentrations of CH_3 and Me_3Si are similar (see Section 4.6), similar quantum yields for these two products are expected, and were observed.

The formation of Me_3SiCH_2 may occur either in a primary process

$$Me_4Si + h\nu \longrightarrow Me_3SiCH_2 + H \quad (V)$$

or by hydrogen abstraction from Me_4Si by a reactive intermediate R

$$R + Me_4Si \longrightarrow RH + Me_3SiCH_2 \quad (5)$$

Channel (V) is supported by the observation of H_2 at high Me_4Si pressure and from the results in the liquid phase [3]. If all H atoms formed in reaction (V) react via channel (5) to give H_2, a maximum quantum yield

$$\Phi(H_2) = \frac{1.8\times10^{-3} + 2.4\times10^{-3}}{2} = 2.1\times10^{-3}$$

at 175 nm is expected. This may be compared with the value of approximately 6×10^{-3} obtained by a rough

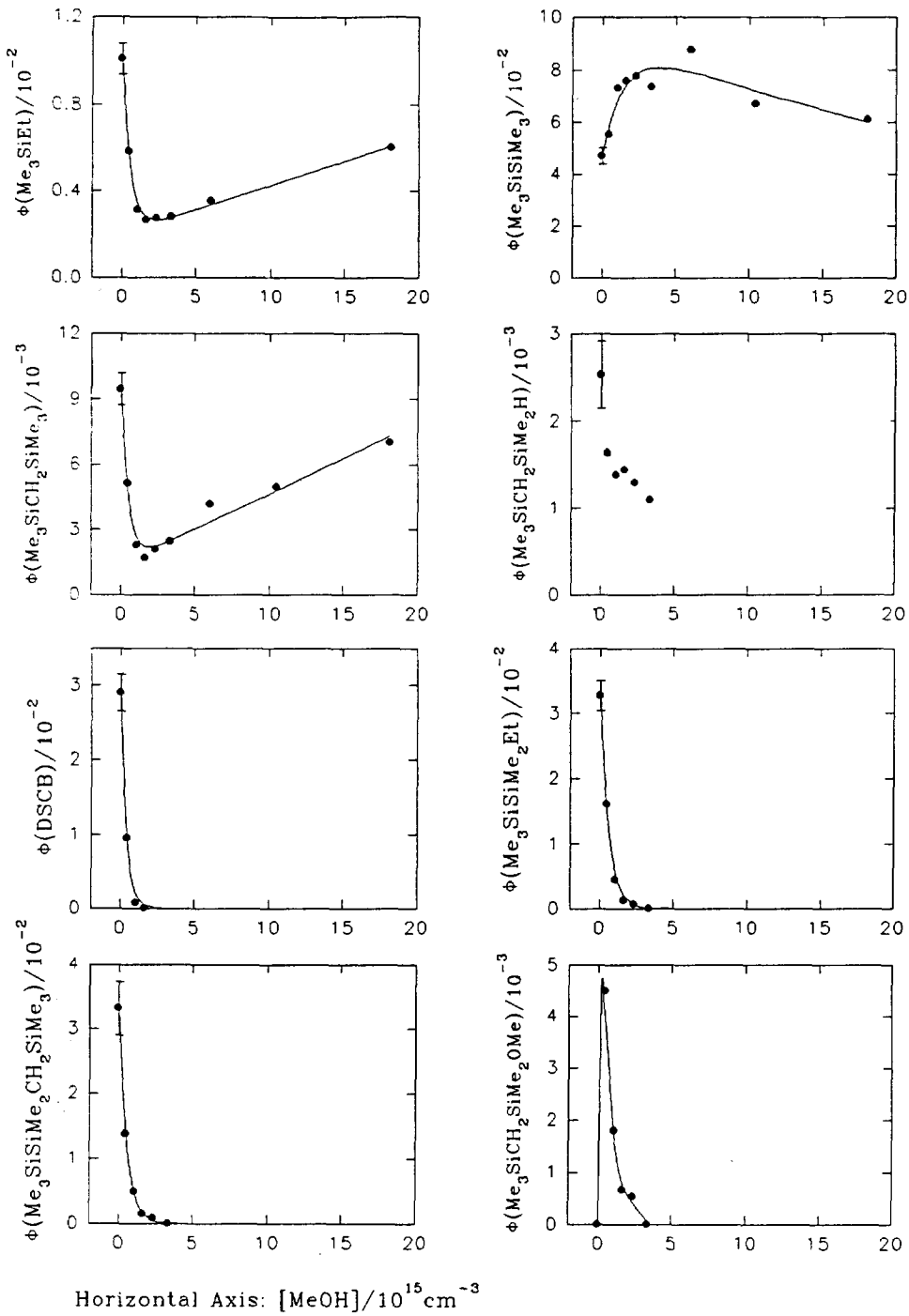

Fig. 7. Dependence of the product quantum yields on MeOH concentration in the 185 nm photolysis of 13.3 mbar Me_4Si.

measurement at 185 nm. Other H atom-forming processes such as

$$Me_4Si + h\nu \longrightarrow Me_2SiCH_2 + H + CH_3 \quad \text{(VI)}$$

require a maximum wavelength of 182 nm and will not be considered further [9,11,12]. The possibility of molecular H_2 elimination with the concomitant formation of a trimethylsilylcarbene also exists. This process is energetically possible but there is no indication that it actually occurs.

4.2. The mechanism

There is no doubt that the primary decomposition channels (I) and (II) are by far the most important. To determine their quantum yields, a reaction mechanism must be set up. From a knowledge of the radical reactions and the reactivity of Me_2SiCH_2, the following may be postulated

$$2CH_3 \longrightarrow C_2H_6 \quad (6)$$

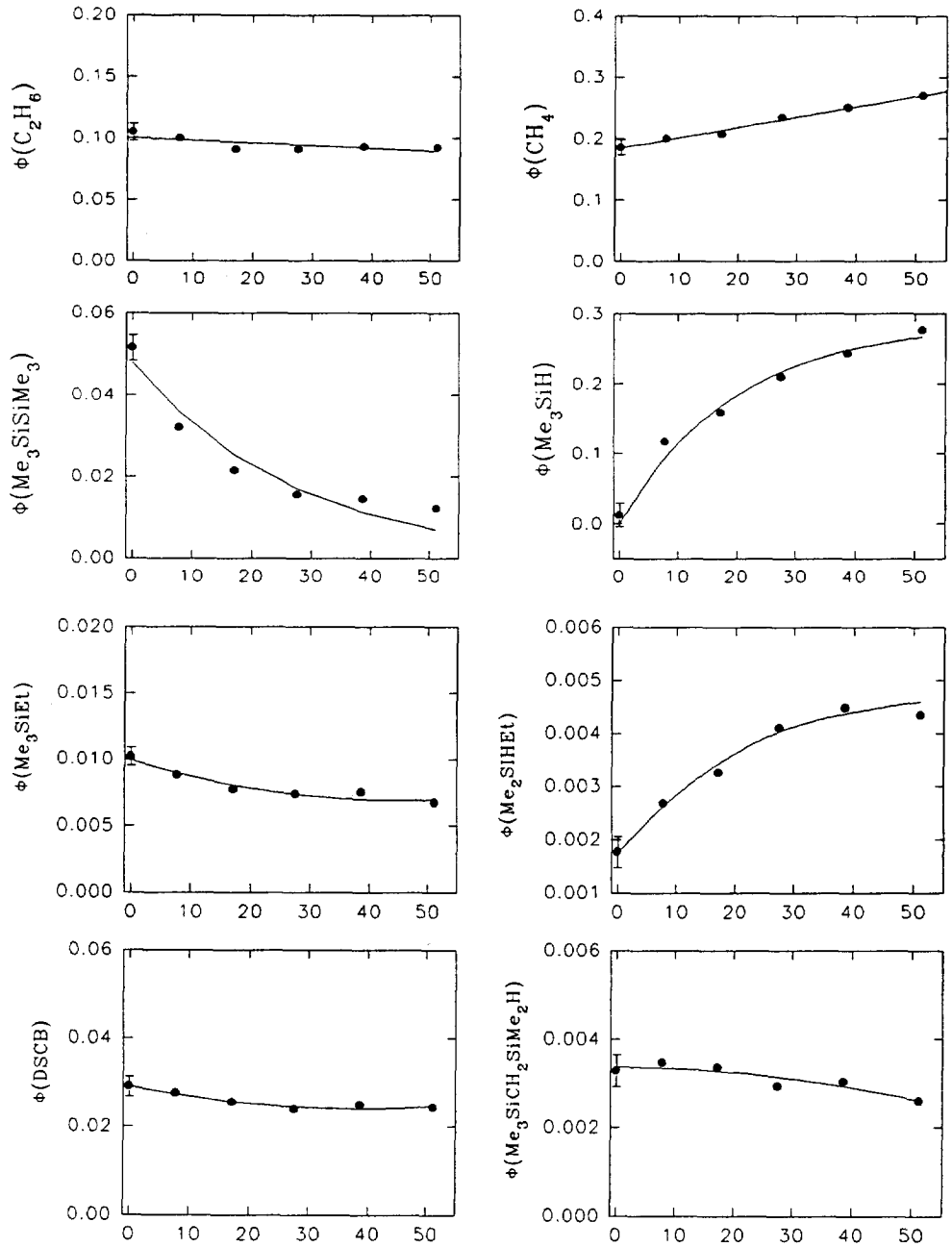

Fig. 8. *(continued)*

$$2Me_3Si \longrightarrow Me_6Si_2 \quad (7)$$

$$Me_3Si + CH_3 \longrightarrow Me_4Si \quad (8)$$

$$2Me_2SiCH_2 \longrightarrow DSCB \quad (9)$$

Reaction (8) cannot be observed directly; however, proof exists that it is actually taking place (Sections 4.4.1 and 4.4.3). The DSCB yield is a factor of three lower than expected, which means that most of the Me_2SiCH_2 must be hidden in other products. With the exception of Me_3SiH, all other products not accounted for by reactions (6)–(9) contain the $-(Me_2SiCH_2)-$ structural unit. In addition, with the exception of Me_2HSiEt and $Me_2HSiCH_2SiMe_3$, all are subject to MeOH scavenging (Figs. 7 and 12). There are only two groups, CH_3 and Me_3Si, which bond to the $-(Me_2SiCH_2)-$ unit, and it was postulated in Ref. [3] that these products are formed by radical addition to Me_2SiCH_2

$$CH_3 + Me_2SiCH_2 \longrightarrow Me_3SiCH_2 \quad (10a)$$

$$CH_3 + Me_2SiCH_2 \longrightarrow Me_2EtSi \quad (10b)$$

$$Me_3Si + Me_2SiCH_2 \longrightarrow Me_3SiSiMe_2CH_2 \quad (11a)$$

$$Me_3Si + Me_2SiCH_2 \longrightarrow Me_3SiCH_2SiMe_2 \quad (11b)$$

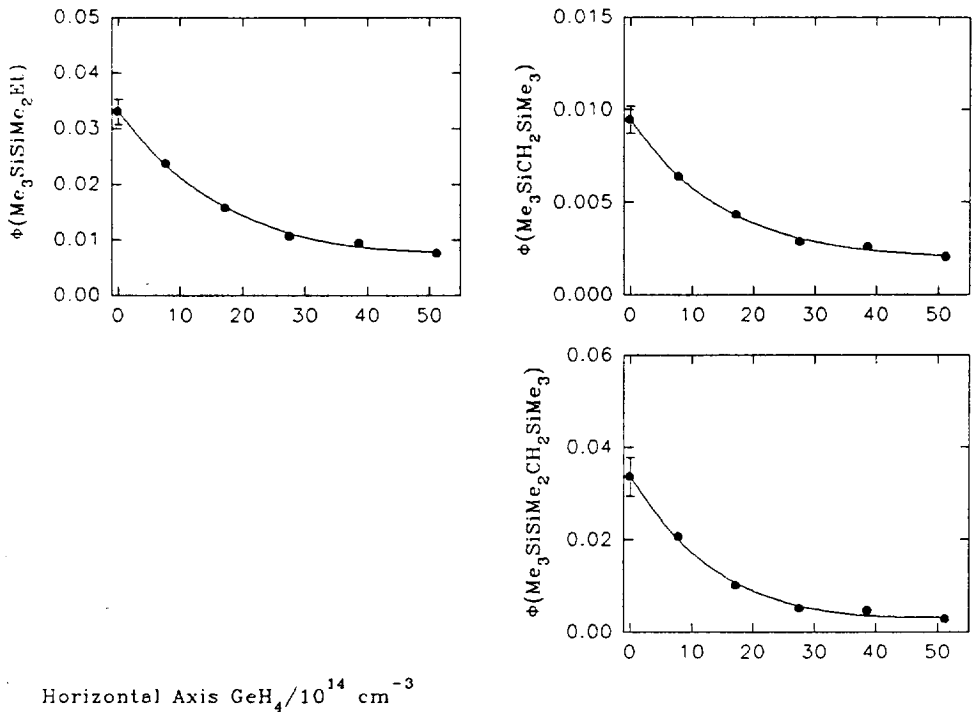

Fig. 8. Dependence of the product quantum yields on GeH_4 concentration in the 185 nm photolysis of 13.3 mbar Me_4Si.

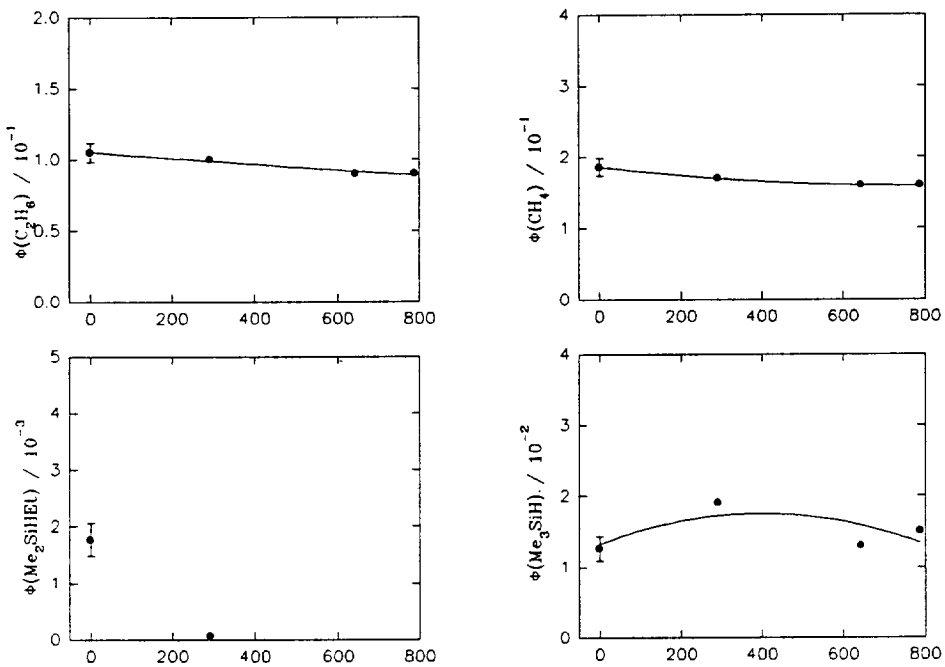

Fig. 9. *(continued)*

$$CH_3 + Me_3SiCH_2 \longrightarrow Me_3SiEt \quad (12)$$

$$CH_3 + Me_2SiEt \longrightarrow Me_3SiEt \quad (13)$$

$$Me_3Si + Me_3SiCH_2 \longrightarrow Me_3SiCH_2SiMe_3 \quad (14)$$

$$CH_3 + Me_3SiCH_2SiMe_2 \longrightarrow Me_3SiCH_2SiMe_3 \quad (15)$$

$$Me_3Si + Me_2EtSi \longrightarrow Me_3SiSiMe_2Et \quad (16)$$

$$CH_3 + Me_3SiSiMe_2CH_2 \longrightarrow Me_3SiSiMe_2Et \quad (17)$$

$$Me_3Si + Me_3SiSiMe_2CH_2 \longrightarrow Me_3SiSiMe_2CH_2SiMe_3 \quad (18)$$

$$Me_3Si + Me_3SiCH_2SiMe_2 \longrightarrow Me_3SiSiMe_2CH_2SiMe_3 \quad (19)$$

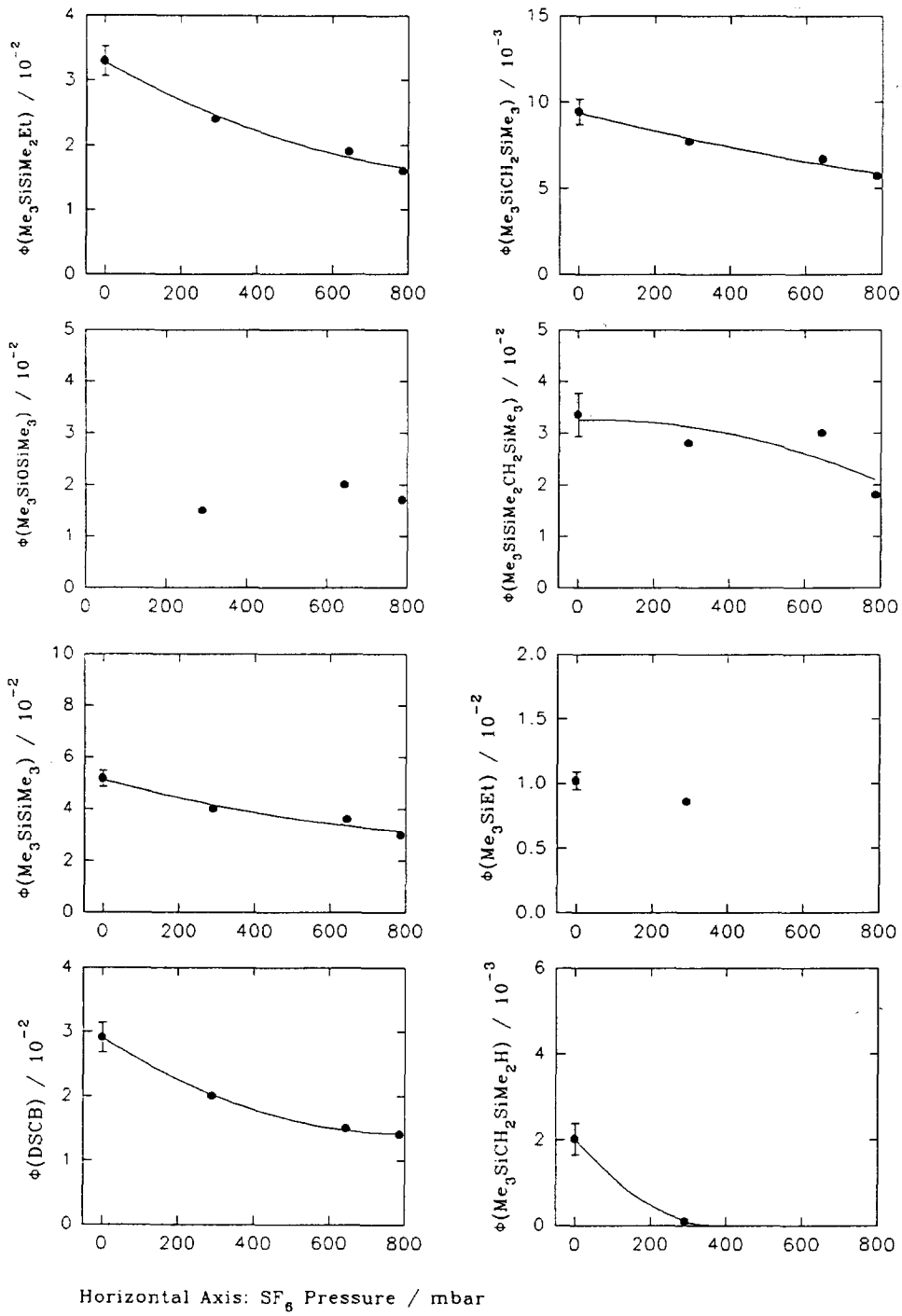

Fig. 9. Dependence of the product quantum yields on SF_6 pressure in the 185 nm photolysis of 13.3 mbar Me_4Si.

Indeed, these products are very sensitive to the presence of NO, but unfortunately this does not prove the participation of radicals because DSCB also disappears rapidly in the presence of NO. However, the experiments with GeH_4 demonstrate the participation of Me_3Si in the formation of some of these products, namely those formed in reactions (14)–(19).

Self- and cross-combination of the radicals formed in reactions (10) and (11) need not be considered, because the corresponding products have not been observed. Because Me_3Si and CH_3 are present in excess, reactions (12)–(19) are favoured.

The mechanism is incomplete because radical–radical disproportionation reactions have not been taken into account. Although the disproportionation of carbon-centred radicals of the type appearing in reactions (6)–(19) cannot occur because of the absence of β-H atoms, disproportionation between carbon–silicon- and

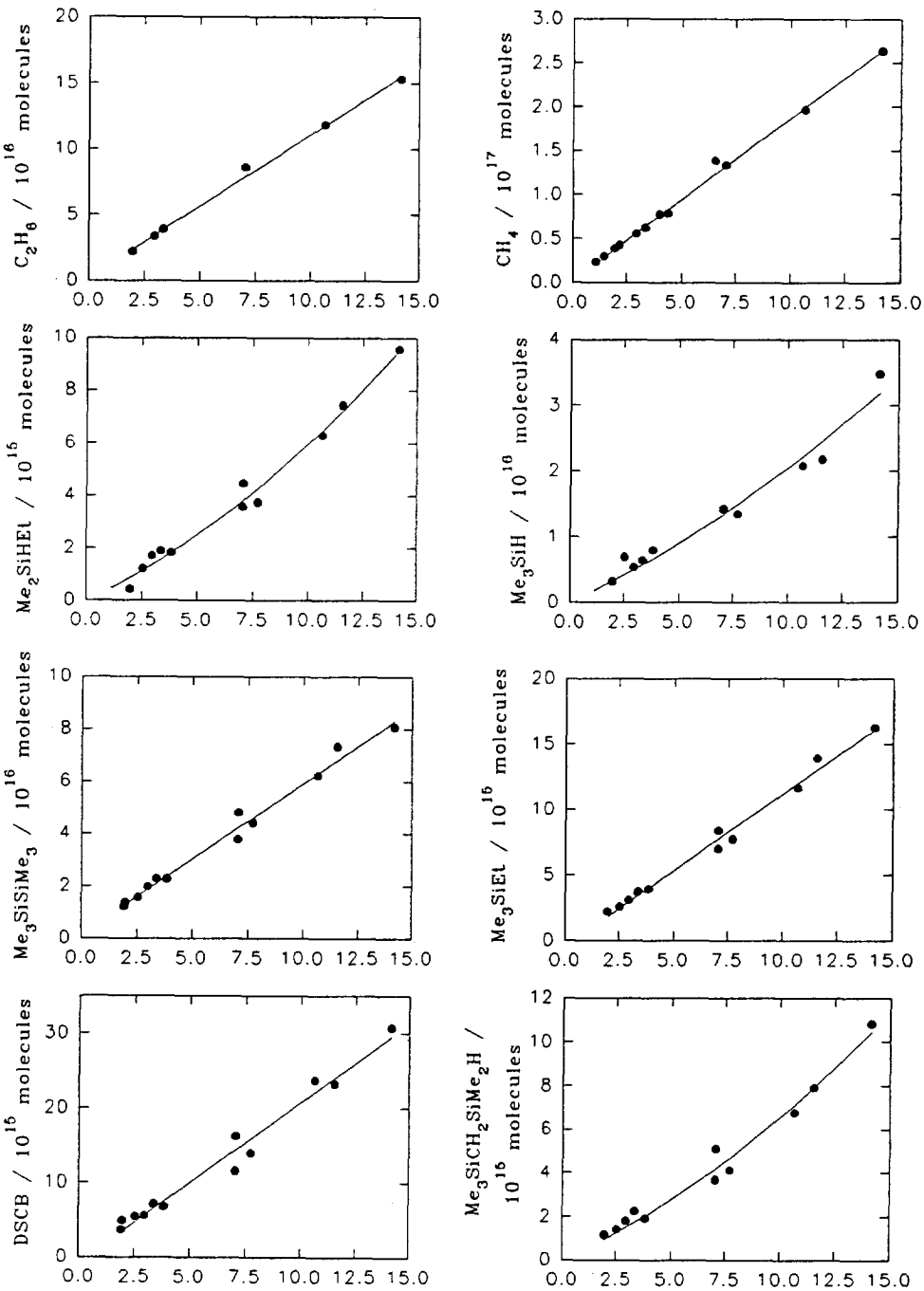

Fig. 10. *(continued)*

silicon–silicon-centred radicals must be taken into consideration.

A number of publications exist concerning the disproportionation to combination ratio of two Me_3Si radicals [2,3,13–18]. In most cases Me_3Si radicals were generated from Me_3SiH. The formation of Me_3SiH in the disproportionation reaction

$$2Me_3Si \longrightarrow Me_3SiH + Me_2SiCH_2 \quad (20)$$

could not be measured directly. To circumvent this problem, the measurement of Me_2SiCH_2 was effected by trapping with MeOH. However, there are problems with this method as has been pointed out by Safarik et al. [18]. More recently, Kerst [19] was able to follow the pathways of Me_2SiCH_2, generated in reaction (20), to stable products, giving $k(20)/k(7) = 0.07 \pm 0.01$. The present system allows the monitoring of the formation of the product Me_3SiH, and so, in principle, a more accurate value for $k(20)/k(7)$ should be obtained. The quantum yield for that part of Me_3SiH which can be quenched by NO is $\Phi(Me_3SiH) = 1.3 \times 10^{-2} - 2.5 \times 10^{-3} = 1.05 \times 10^{-2}$ at 185 nm and 1.95×10^{-2} at 175

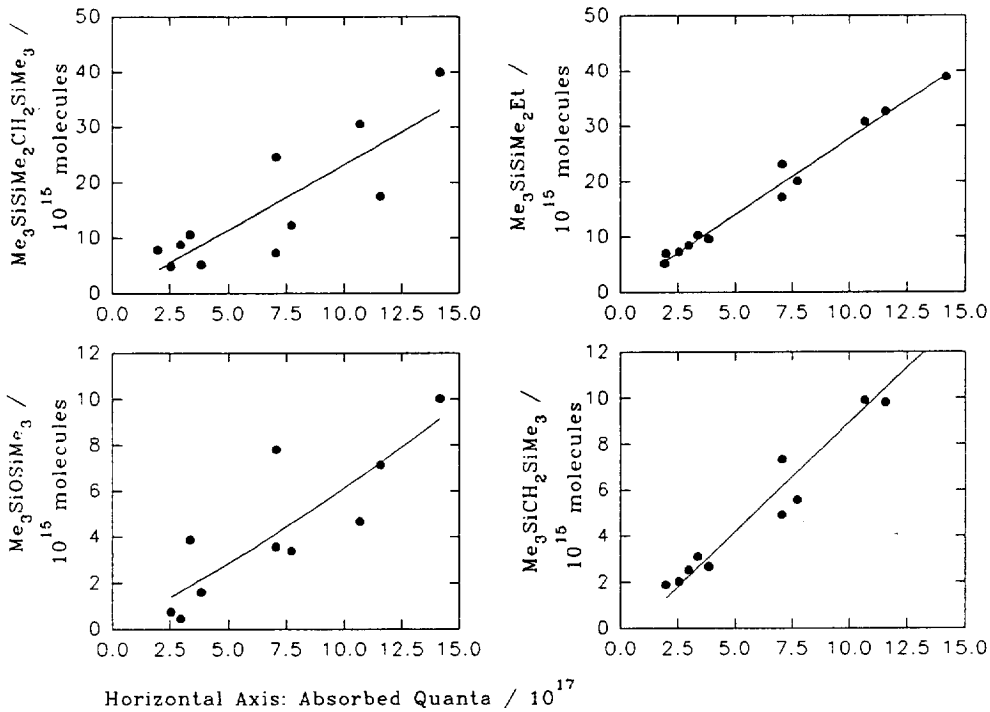

Fig. 10. Dependence of the product yields on the number of absorbed quanta in the 175 nm photolysis of 13.3 mbar Me_4Si.

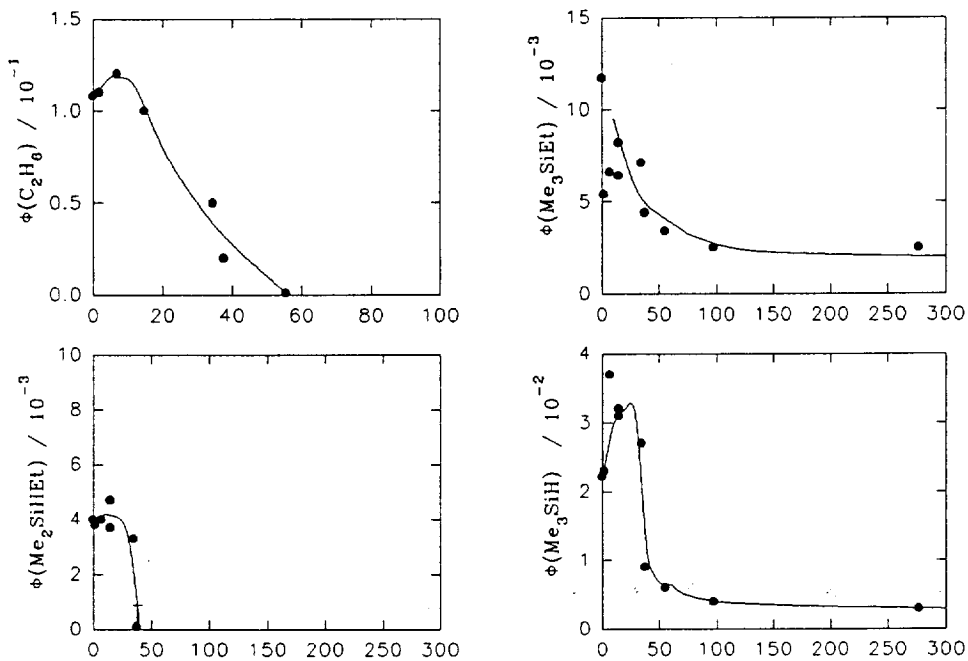

Fig. 11. *(continued)*

nm. These values, together with the quantum yield for Me_6Si_2, give $k(20)/k(7) = 0.20$ at 185 nm and 0.34 at 175 nm. Both values are much higher than the literature values referred to above and, in addition, are wavelength dependent. Therefore other processes must contribute to the Me_3SiH quantum yield. Other possible sources of Me_3SiH may be contributions from disproportionation reactions other than reaction (20). The disproportionation reactions associated with reactions (16) and (19) belong to this class

$$Me_2EtSi + Me_3Si \longrightarrow Me_3SiH + MeEtSiCH_2 \quad (21a)$$

$$Me_2EtSi + Me_3Si \longrightarrow Me_3SiH + Me_2SiCHCH_3 \quad (21b)$$

$$Me_2EtSi + Me_3Si \longrightarrow Me_2EtSiH + Me_2SiCH_2 \quad (22)$$

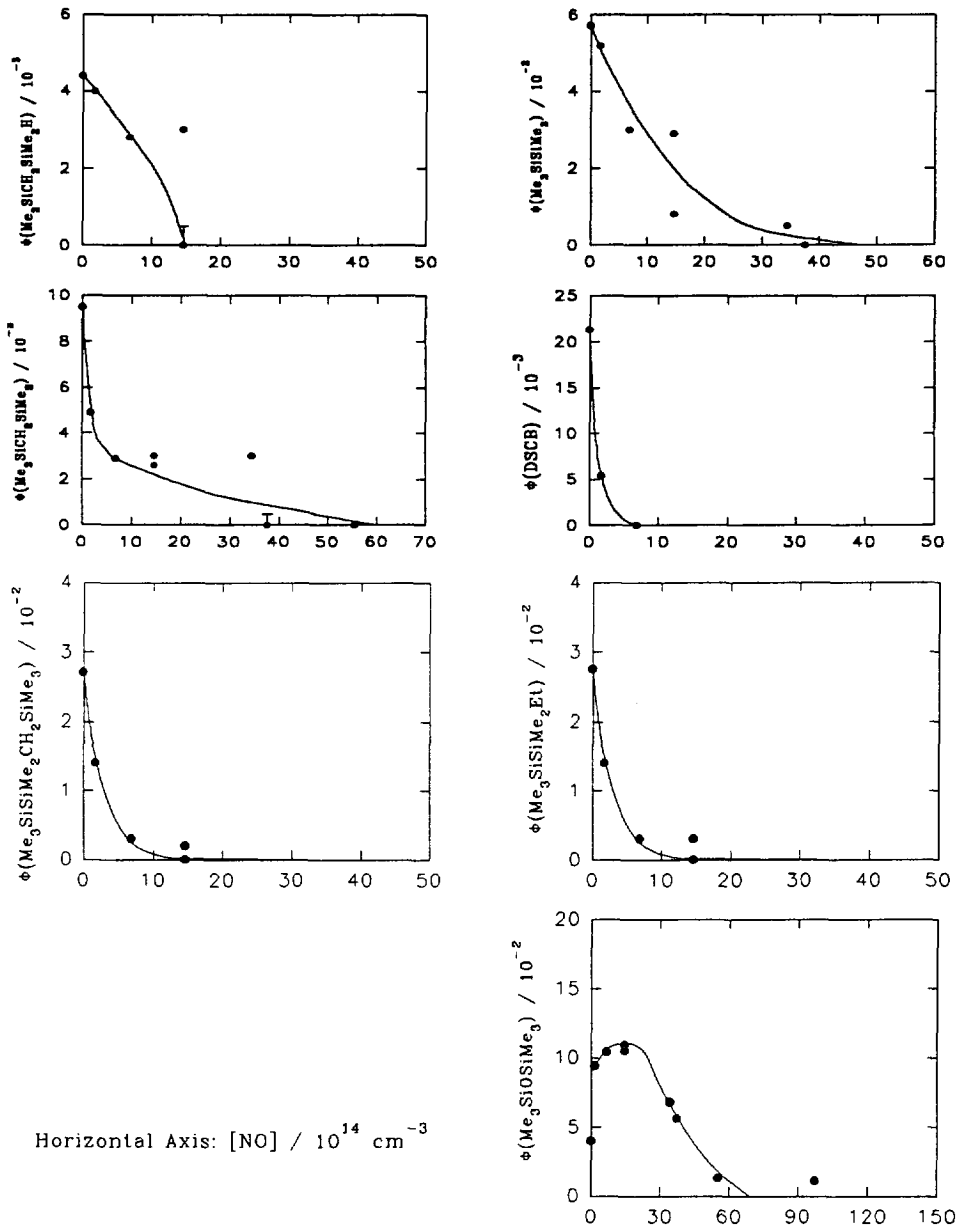

Fig. 11. Dependence of the product quantum yields on NO concentration in the 175 nm photolysis of 13.3 mbar Me_4Si.

$$Me_3SiCH_2SiMe_2 + Me_3Si \longrightarrow Me_3SiH + Me_3SiCH_2SiMeCH_2 \quad (23a)$$

$$Me_3SiCH_2SiMe_2 + Me_3Si \longrightarrow Me_3SiH + Me_3SiCHSiMe_2 \quad (23b)$$

$$Me_3SiCH_2SiMe_2 + Me_3Si \longrightarrow Me_3SiCH_2SiMe_2H + Me_2SiCH_2 \quad (24)$$

All three stable products of reactions (21)–(24) were indeed observed, but none of these products showed a dependence on MeOH (Fig. 12). Therefore it must be concluded that reactions (21)–(24) do not take place. Other disproportionation reactions which should be considered are

$$CH_3 + Me_3Si \longrightarrow CH_4 + Me_2SiCH_2 \quad (25)$$

$$CH_3 + Me_2EtSi \longrightarrow CH_4 + MeEtSiCH_2 \quad (26a)$$

$$CH_3 + Me_2EtSi \longrightarrow CH_4 + Me_2SiCHCH_3 \quad (26b)$$

$$CH_3 + Me_3SiCH_2SiMe_2 \longrightarrow CH_4 + Me_3SiCH_2SiMeCH_2 \quad (27a)$$

$$CH_3 + Me_3SiCH_2SiMe_2 \longrightarrow CH_4 + Me_3SiCHSiMe_2 \quad (27b)$$

If these reactions contribute to the CH_4 yield, the CH_4 yield should decrease with the addition of NO. A least-squares treatment of the data in Fig. 6 shows a small

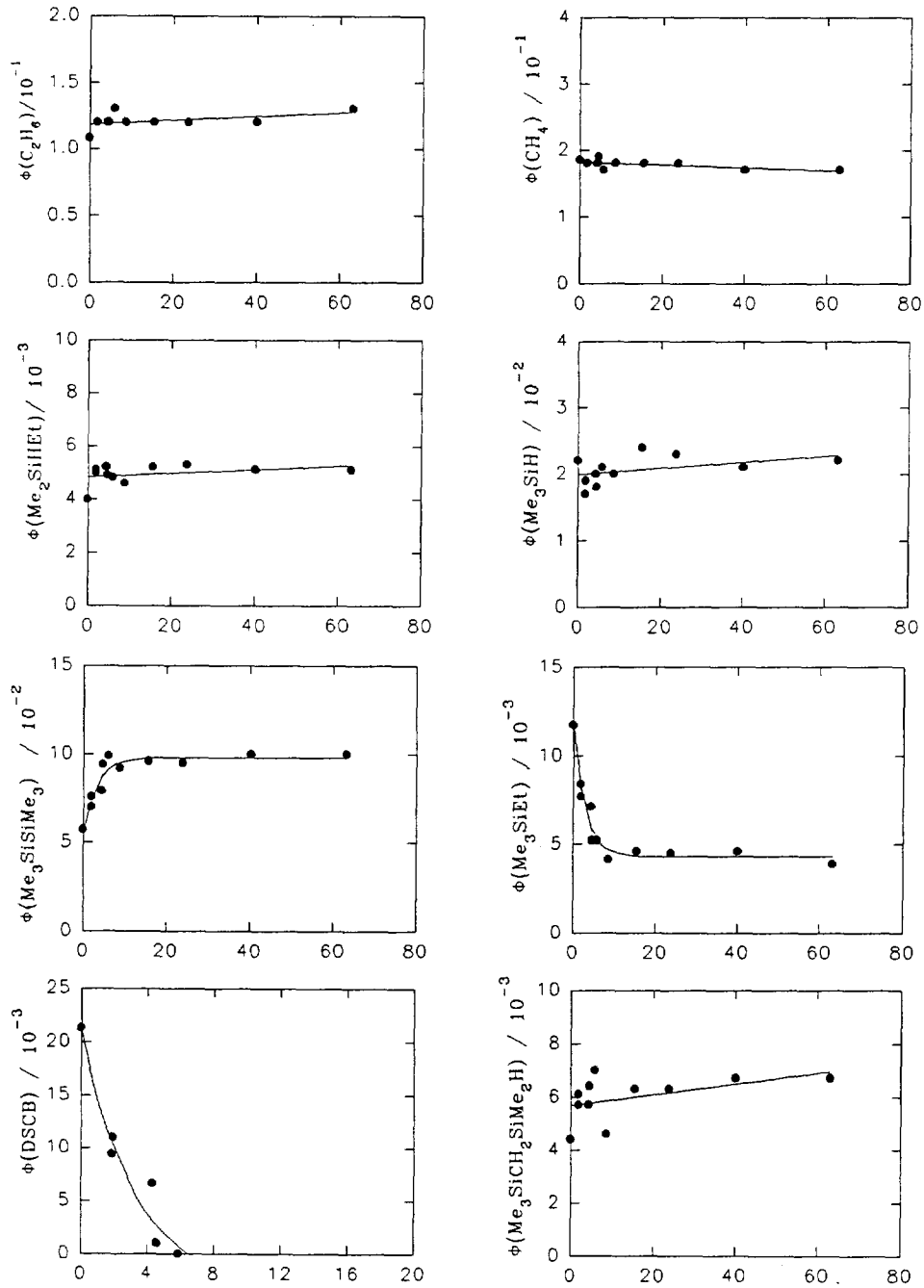

Fig. 12. (*continued*)

decrease: the slope is $-(2.7\pm6.7)\times10^{-18}$ cm^3. At an NO concentration of 5×10^{15} cm^{-3}, Me_6Si_2 has completely disappeared, and therefore reaction (25) should also have ceased. A decrease in $\Delta\Phi(CH_4)$ of -0.016 ± 0.041 was calculated. As will be shown in Section 4.4.3, the quantum yield of Me_4Si formation by reaction (8) is $\Phi(Me_4Si)=0.19$, and therefore $k(25)/k(8)\leqslant0.08\pm0.18$. This value is very much smaller than the literature value obtained from a similar complex system [20]. From these results, it is concluded that disproportionation reactions leading to Si=C double bonded species occur only with a small cross-section.

Taking the other minor primary processes into account leads to a further expansion of the mechanism. If channel (IVa) is responsible for the non-scavengeable portion of Me_3SiH and Me_3SiEt, an insertion reaction may be postulated analogous to methylene reactions with alkanes

$$^1CH_2 + Me_4Si \longrightarrow Me_3SiEt \quad (1)$$

in competition with a deactivation step

$$^1CH_2 + Me_4Si \longrightarrow {}^3CH_2 + Me_4Si \quad (28)$$

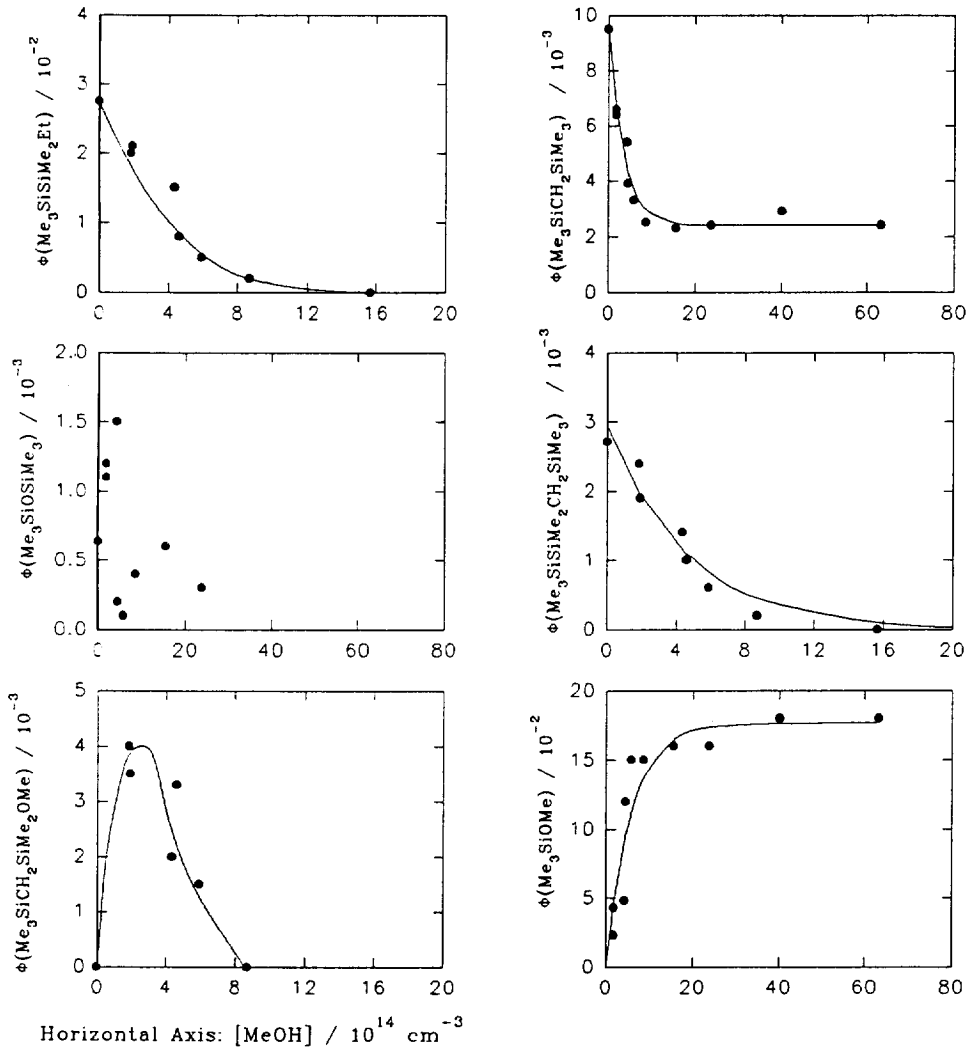

Fig. 12. Dependence of the product quantum yields on MeOH concentration in the 175 nm photolysis of 13.3 mbar Me_4Si.

The $^3CH_2$ will probably then be transferred to stable products by reaction with the radicals present. Reaction (1) must be very fast not to be influenced by the addition of NO, which is actually the case [21], and the deactivation step must be slow not to change the 1 : 1 ratio between the Me_3SiH and Me_3SiEt yields in the presence of NO. Experiments with additives, such as SF_6, which deactivate $^1CH_2$ quite effectively [22] were not precise enough to allow an unambiguous decision for or against the occurrence of $^1CH_2$ in this system.

For the hydrogen atoms formed in channel (V), the following reactive pathways are open

$$H + Me_4Si \longrightarrow Me_3SiCH_2 + H_2 \quad (29)$$

$$H + Me_3Si \longrightarrow Me_3SiH \quad (30)$$

$$H + CH_3 + M \longrightarrow CH_4 + M \quad (31)$$

$$H + Me_2SiCH_2 \longrightarrow Me_2HSiCH_2,\ Me_3Si \quad (32)$$

To account for the previously unexplained products, $Me_2HSiCH_2SiMe_3$ and Me_2HSiEt, reaction (32), followed by reactions (33) and (34), was postulated in a previous publication [3]

$$Me_2HSiCH_2 + Me_3Si \longrightarrow Me_2HSiCH_2SiMe_3 \quad (33)$$

$$Me_2HSiCH_2 + CH_3 \longrightarrow Me_2HSiCH_2CH_3 \quad (34)$$

However, from our scavenger experiments with MeOH (Fig. 12), we must conclude that reactions (32)–(34) do not account for the formation of these two products.

In addition to Me_2HSiEt and $Me_2HSiCH_2SiMe_3$, major portions of Me_3SiH have not yet been accounted for by the mechanism. These three products show a clear increase in their quantum yields with decreasing irradiation wavelength (Table 1). The larger than anticipated value for Me_3SiH at 193 nm is due to secondary photolysis. Therefore, it is tempting to assume that the excess energy imparted by the photons plays an important role in the formation of these three products. At 175 nm, the photon energy exceeds the Si–C bond dissociation energy by 300 kJ mol^{-1}. This excess energy will be distributed among the various degrees of freedom

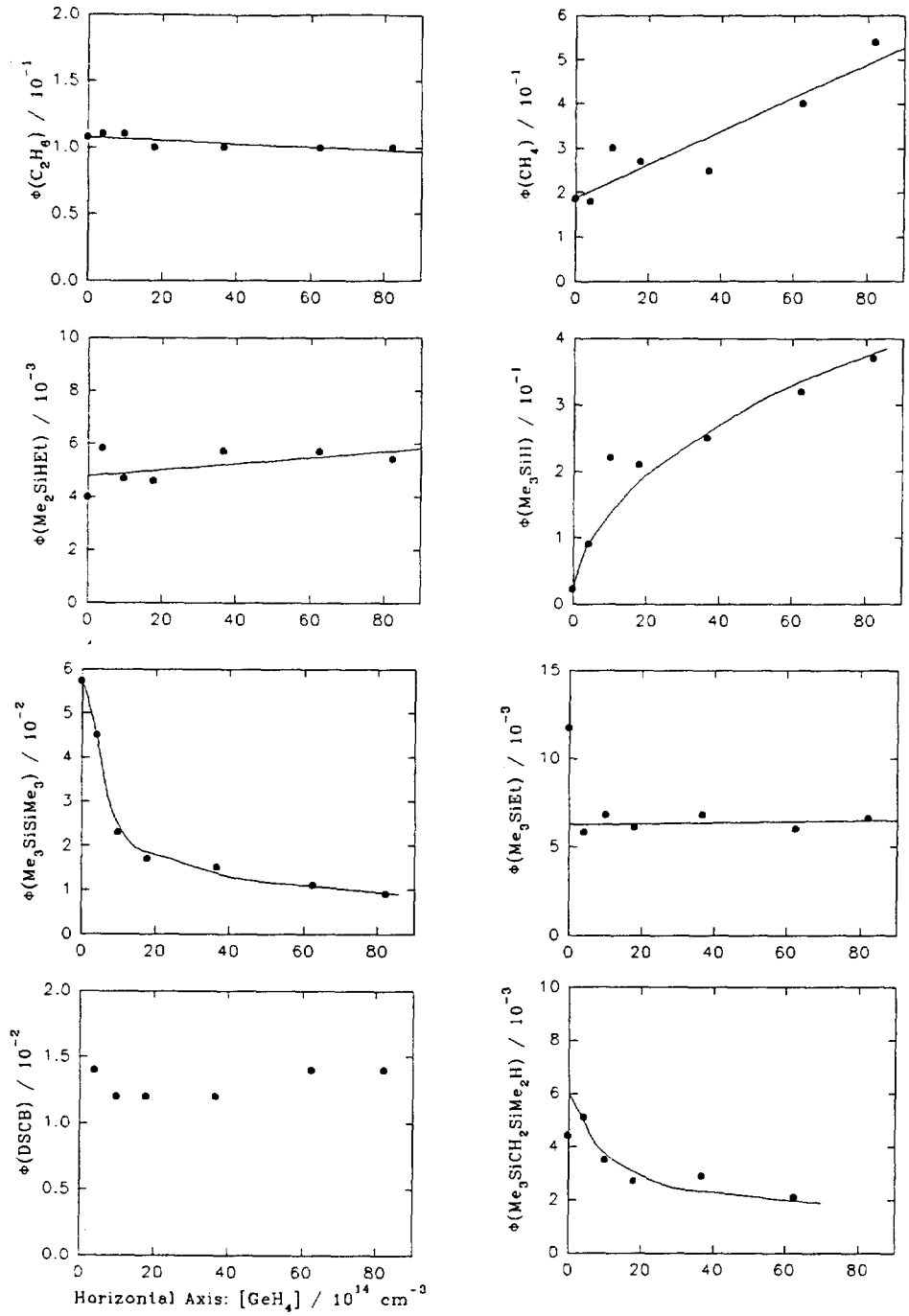

Fig. 13. Dependence of the product quantum yields on GeH_4 concentration in the 175 nm photolysis of 13.3 mbar Me_4Si.

of the two decomposition products. If the ergodicity assumption is also valid for the photoactivated molecule, the excess energy should be distributed uniformly among the active degrees of freedom of the activated complex. Assuming a Gorin-type transition state with five free internal rotations, an effective number of classical oscillators $s_{eff}=5.5$ in the Me_3Si group and a negligibly small number for the CH_3 group, it may be concluded that Me_3Si carries away

$$\frac{5.5}{(5.5+1+5)}\,300 \approx 150 \text{ kJ mol}^{-1}$$

as internal vibrational energy with the concomitant formation of an essentially thermalized CH_3 radical.

Gammie et al. [1] have proposed that such hot radicals are responsible for a number of reactions quite unlikely to occur with thermalized radicals. Certainly the excess

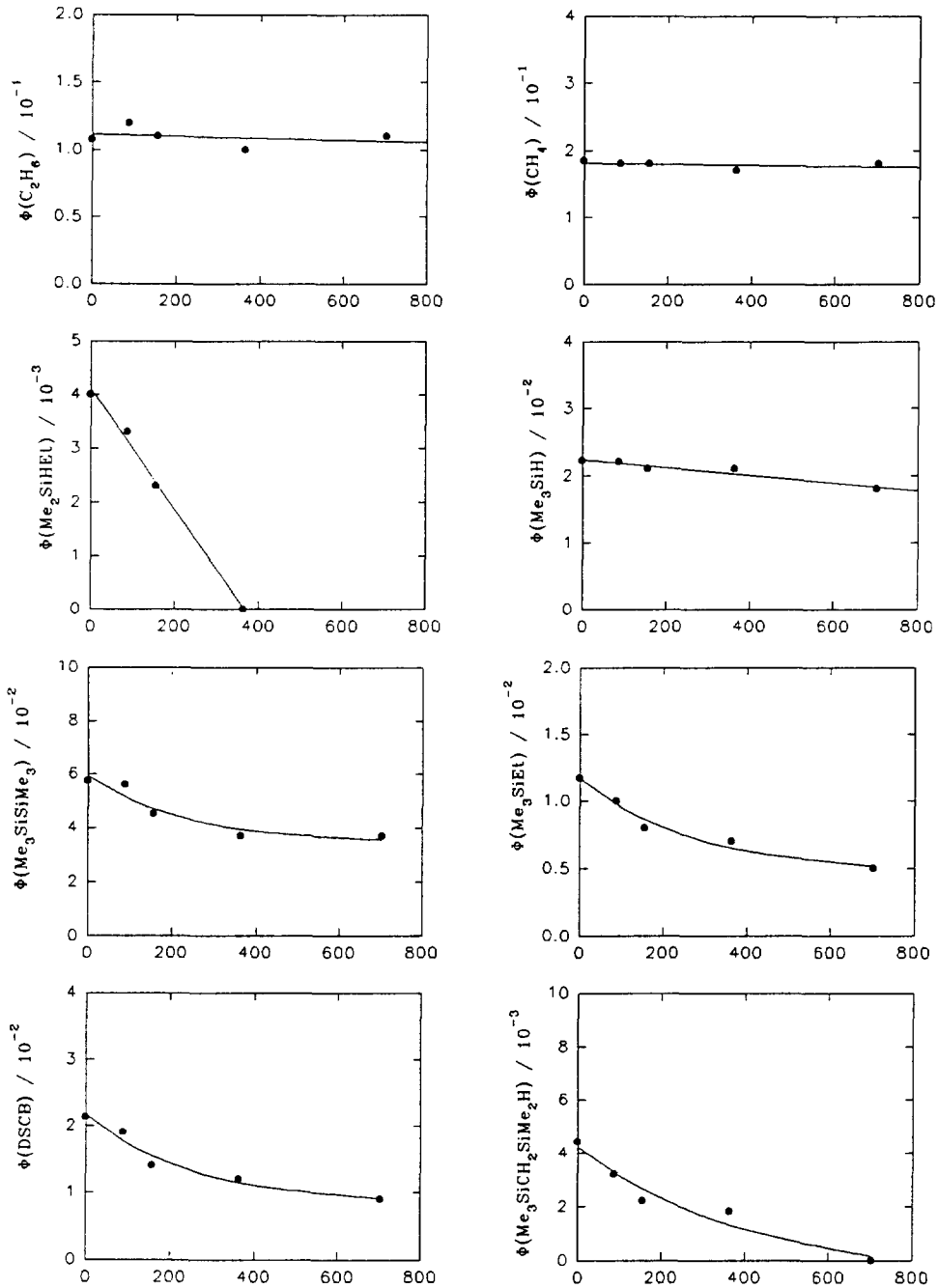

Fig. 14. (*continued*)

energy in the Me_3Si radical (Me_3Si^v) is much greater than the activation energy for hydrogen abstraction from Me_4Si. Therefore

$$Me_3Si^v + Me_4Si \longrightarrow Me_3SiH + Me_3SiCH_2 \quad (35)$$

must be considered. Despite the high vibrational excitation, reaction (35) does not occur simply because there is no room left for more Me_3SiCH_2 radicals in the material balance. Only if primary process (V) is dismissed and the observed H_2 yield is attributed totally to secondary formation could there be a maximum quantum yield $\Phi(35) = 4.2 \times 10^{-3}$. It cannot be stated with certainty that reaction (35) does not occur, but certainly the sum of the quantum yields $\phi(V) + \Phi(29) + \Phi(35)$ must not exceed the value 4.2×10^{-3}. In any case it may be concluded that reaction (35) is an unimportant process. This conclusion should not be too astonishing because the energy resides in the wrong part of the collision complex. Even if reaction (35) did take place, it would still not resolve the Me_3SiH deficiency problem. According to this proposed mechanism

$$\Phi(Me_3SiH) = \Phi(IV) + \Phi(20) + \Phi(30) \text{ or } \Phi(35)$$

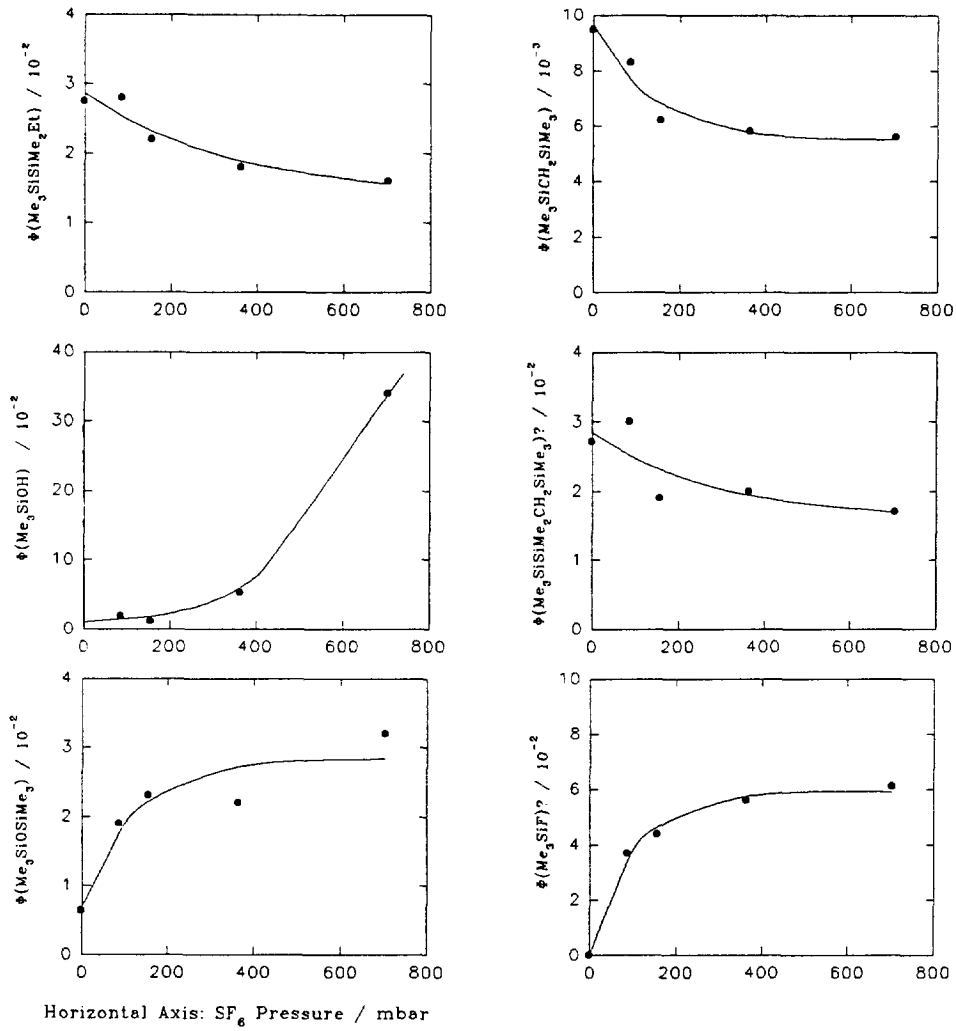

Fig. 14. Dependence of the product quantum yields on SF_6 concentration in the 175 nm photolysis of 13.3 mbar Me_4Si.

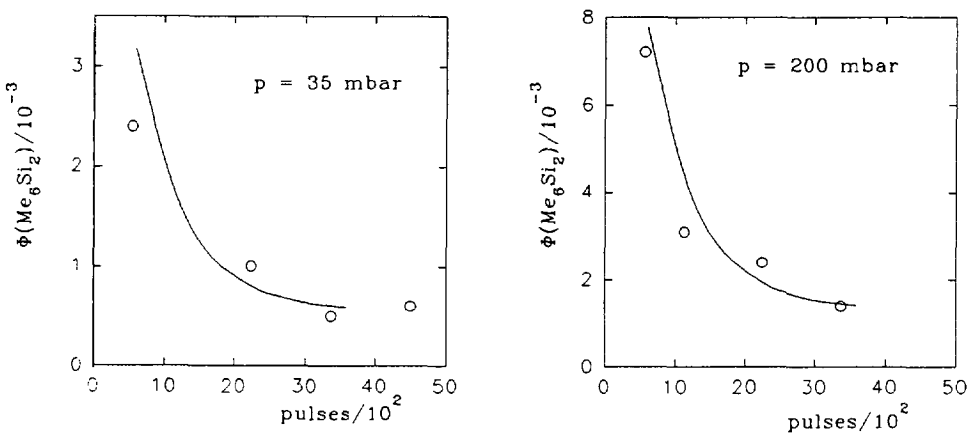

Fig. 15. Dependence of the Me_6Si_2 quantum yield on the number of laser pulses at 193 nm: symbols, experimental points; line, calculated (see text).

Because of the competition of reaction (30) with reactions (29), (31) and (32), $\Phi(30)$ will be smaller than $\Phi(35)$. Thus only an upper limit to $\Phi(Me_3SiH)$ can be assigned

$$\Phi(Me_3SiH) \leqslant 2.5\times10^{-3} + 0.07\Phi(Me_6Si_2) + 4.2\times10^{-3} \leqslant 10.7\times10^{-3}$$

This upper limit is not too far from the experimental

value at 185 nm, but is lower by a factor of two at 175 nm. To rationalize that part of $\Phi(Me_3SiH)$ which is not accounted for by the mechanism, it is postulated that the ratio of disproportionation to recombination is larger for vibrationally excited silyl radicals than for thermalized radicals.

$$2Me_3Si^{v} \longrightarrow Me_3SiH + Me_2SiCH_2 \quad (36)$$

The ratio of disproportionation to combination of hot Me_3Si radicals at 175 nm is $0.27 \leqslant k(36)/k(7) \leqslant 0.32$. This is approximately four times larger than the ratio of thermalized Me_3Si radicals, $k(20)/k(7) = 0.07$. A similar phenomenon is observed in the case of alkyl radicals [23].

The final task is to propose a mechanism for the formation of Me_2HSiEt and $Me_2HSiCH_2SiMe_3$. As has been noted already, reactions (32)–(34) are not able to explain these two products. An alternative could be reactions (12) and (13) followed by

$$Me_2EtSi + Me_4Si \longrightarrow Me_2EtSiH + Me_3SiCH_2 \quad (37)$$

$$Me_3SiCH_2SiMe_2 + Me_4Si \longrightarrow Me_2HSiCH_2SiMe_3 + Me_3SiCH_2 \quad (38)$$

These two reactions are endothermic by about 30–35 kJ mol^{-1} [24] and can occur only if the two radicals are activated. In the case of reactions (12) and (13), an Si=C π bond is broken and, in its place, C–C and C–Si bonds are formed. The exothermicity and therefore the excitation of the silyl radical is approximately 225 kJ mol^{-1} with $\Delta H^{\circ}(Si-C) \approx \Delta H^{\circ}(C-C) \approx 375$ kJ mol^{-1} [24,25] and $B_{\pi} \approx 150$ kJ mol^{-1} [12]. Again, reactions (37) and (38) do not play a significant role despite the large excitation energy as can be deduced from the MeOH experiments (Fig. 12). The reason is probably the same as in the case of reaction (35). If the formation of these two products does not proceed via Me_2SiCH_2, either another primary process or an energy-rich precursor is needed to allow the formation of an Si–H bond at the expense of a C–H bond. Isomerization of the vibrationally excited Me_3Si radical is a possibility

$$Me_3Si^{v} \longleftrightarrow Me_2HSiCH_2^{v} \quad (39, -39)$$

$$Me_2HSiCH_2^{v} + M \longrightarrow Me_2HSiCH_2 + M \quad (40)$$

Reaction (39) will be endothermic by about 25–30 kJ mol^{-1} and also will be loaded with an appreciable activation energy. A reaction similar to the back reaction (−39) has been investigated by Davidson et al. [26]. The main difference was that the CH_2 group was inserted into an Si–Si bond rather than an Si–H bond. An activation energy of 90 kJ mol^{-1}, which must be added to the endothermicity of reaction (39), was measured for that process. In these experiments reactions (39) and (40) cannot be distinguished from the formation of the dimethylsilylmethyl radical in a primary process.

4.3. Material balance

The most likely mechanism is shown in condensed form in Table 2. From this mechanism, the quantum yield of the primary process (I) is given by

$$\Phi(I) = \Phi(CH_4) - (\Phi(25) + \Phi(26) + \Phi(27))$$

$$\Phi(25) + \Phi(26) + \Phi(27) = \Phi(CH_4) - \Phi(CH_4/NO)$$

The quantum yield values for the different processes are also given in Table 2.

The quantum yield of Me_2SiCH_2 formation is given by

$$\Phi(Me_2SiCH_2) = \Phi(I) + \Phi(20)$$

$$\Phi(20) = \Phi(Me_3SiH) - \Phi(IVa) - \Phi(30)$$

$$\Phi(30) = \Phi(V) - \Phi(29)$$

$$\Phi(IVa) = \Phi(Me_3SiH/NO)$$

$$\Phi(V) = \Phi(Me_3SiEt/MeOH) - \Phi(Me_3SiEt/NO) + \Phi(Me_3SiCH_2SiMe_3/MeOH) - \Phi(H_2)$$

Because it has been shown that H_2 is a product only at high Me_4Si pressure, and no quantitative results were obtained, the following apply

$$\Phi(V) = a[\Phi(Me_3SiEt/MeOH) - \Phi(Me_3SiEt/NO) + \Phi(Me_3SiCH_2SiMe_3/MeOH)]$$

with $0.5 \leqslant a \leqslant 1.0$

$$\Phi(29) = \frac{1-a}{a}\Phi(V)$$

$$\Phi(30) = \frac{2a-1}{a}\Phi(V)$$

$$\Phi(Me_2SiCH_2) = \Phi(I) - \Phi(IVa) + \frac{1-2a}{a}\Phi(V) + \Phi(Me_3SiH) \quad (41)$$

The quantum yield of Me_2SiCH_2 formation must be equal to the quantum yield of "Me_2SiCH_2" products

$$\Phi(Me_2SiCH_2) = 2\Phi(DSCB) + \Phi(Me_3SiEt) - \Phi(Me_3SiEt/MeOH) + \Phi(Me_3SiSiMe_2Et) + \Phi(Me_3SiCH_2SiMe_3) - \Phi(Me_3SiCH_2SiMe_3/MeOH) + \Phi(Me_3SiSiMe_2CH_2SiMe_3) \quad (42)$$

The quantum yield of primary process (II) is given by

Table 2
Mechanism and quantum yields for a few selected processes

Reaction number	Reaction	Φ(185 nm)/10^{-2}	Φ(175 nm)/10^{-2}
(I)	$Me_4Si + h\nu \rightarrow CH_4 + Me_2SiCH_2$	17.0 ± 4.1	16.9 ± 4.1
(II)	$Me_4Si + h\nu \rightarrow CH_3 + Me_3Si$	45 ± 5	
(IVa)	$Me_4Si + h\nu \rightarrow {}^1CH_2 + Me_3SiH$	0.25	0.25
(V)	$Me_4Si + h\nu \rightarrow H + Me_3SiCH_2$	$0.08 \leqslant \Phi \leqslant 0.17$	$0.22 \leqslant \Phi \leqslant 0.43$
(6)	$2CH_3 \rightarrow C_2H_6$		
(7)	$2Me_3Si \rightarrow Me_6Si_2$		
(8)	$CH_3 + Me_3Si \rightarrow Me_4Si$		
(9)	$2Me_2SiCH_2 \rightarrow$ DSCB		
(10, 12, 13)	$2CH_3 + Me_2SiCH_2 \rightarrow Me_3SiEt$		
(10, 11, 14, 15, 16, 17)	$CH_3 + Me_3Si + Me_2SiCH_2 \rightarrow Me_3SiSiMe_2Et$, $Me_3SiCH_2SiMe_3$		
(11, 18, 19)	$2Me_3Si + Me_2SiCH_2 \rightarrow Me_3SiSiMe_2CH_2SiMe_3$		
(12)	$CH_3 + Me_3SiCH_2 \rightarrow Me_3SiEt$		
(14)	$Me_3Si + Me_3SiCH_2 \rightarrow Me_3SiCH_2SiMe_3$		
(20)	$2Me_3Si \rightarrow Me_3SiH + Me_2SiCH_2$	1.0 ± 0.2	1.75 ± 0.2
(25, 26, 27)	$CH_3 + R_3Si \rightarrow CH_4 + R_3Si(-H)$	1.6 ± 4.1	
(1)	${}^1CH_2 + Me_4Si \rightarrow Me_3SiEt$		
(28)	${}^1CH_2 + Me_4Si \rightarrow {}^3CH_2 + Me_4Si$		
(29)	$H + Me_4Si \rightarrow H_2 + Me_3SiCH_2$	$0.08 \geqslant \Phi \geqslant 0.0$	$0.22 \geqslant \Phi \geqslant 0.0$
(30)	$H + Me_3Si \rightarrow Me_3SiH$	$0.0 \leqslant \Phi \leqslant 0.17$	$0.0 \leqslant \Phi \leqslant 0.43$
(39)	$Me_3Si \rightarrow Me_2HSiCH_2$	0.38 ± 0.05	0.88 ± 0.07
(33)	$Me_2HSiCH_2 + Me_3Si \rightarrow Me_2HSiCH_2SiMe_3$		
(34)	$Me_2HSiCH_2 + CH_3 \rightarrow Me_2HSiEt$		
(41)	$\Phi(Me_2SiCH_2)$	18.0 ± 4.1	18.7 ± 4.1
(42)	$\Phi(Me_2SiCH_2)$	14.1 ± 0.7	12.9 ± 0.4
	$\Phi(CH_3) - \Phi(8)$	28.5 ± 4.3	28.7 ± 4.1
	$\Phi(Me_3Si) - \Phi(8)$	25.4 ± 4.3	27.0 ± 4.2

$$\Phi(II) = \Phi(CH_3) = \Phi(Me_3Si)$$

$$\begin{aligned}\Phi(CH_3) = {} & 2\Phi(C_2H_6) + \Phi(Me_4Si) + 2[\Phi(Me_3SiEt) \\ & - \Phi(Me_3SiEt/MeOH)] \\ & + \Phi(Me_3SiEt/MeOH) - \Phi(Me_3SiEt/NO) \\ & + \Phi(Me_3SiSiMe_2Et) \\ & + \Phi(Me_3SiCH_2SiMe_3) \\ & - \Phi(Me_3SiCH_2SiMe_3/MeOH) \\ & + \Phi(CH_4) - \Phi(CH_4/NO) \\ & + \Phi(Me_2HSiEt) \end{aligned} \quad (43)$$

$$\begin{aligned}\Phi(Me_3Si) = {} & 2\Phi(Me_6Si_2) + \Phi(Me_4Si) \\ & + \Phi(Me_3SiSiMe_2Et) \\ & + \Phi(Me_3SiCH_2SiMe_3) \\ & + 2\Phi(Me_3SiSiMe_2CH_2SiMe_3) \\ & + 2[\Phi(Me_3SiH) - \Phi(IVa)] \\ & - [(2a-1)/a]\Phi(V) + \Phi(Me_2HSiEt) \\ & + 2\Phi(Me_2HSiCH_2SiMe_3) \end{aligned} \quad (44)$$

Although Φ(I) is given essentially by the CH_4 quantum yield, contributions from processes (25), (26) and (27), while very small, introduce a very large error into Φ(I). At 175 nm, $\Phi(25) + \Phi(26) + \Phi(27)$ has not been determined, so the 185 nm value has been taken. No dependence of Φ(I) on wavelength can be discerned.

The quantum yield of Me_2SiCH_2 formation comes from two contributions, process (I) and reaction (20). To calculate Φ(20), Φ(IVa) and Φ(V) must be known. The part of $\Phi(Me_3SiH)$ which cannot be scavenged by NO is Φ(IVa) and represents a very small contribution to the total decomposition quantum yield. For Φ(V), only a lower and upper limit can be given; the value is very small but it depends strongly on the photolysis wavelength. For the evaluation of Φ(20), which also depends on the photolysis wavelength, a mean value of Φ(V) has been used. At 185 nm, 78% and, at 175 nm, 69% of the Me_2SiCH_2 is recovered in the products (reaction (42)). The rest elude detection either because of polymer formation or wall adsorption.

The quantum yield of (II) can be determined in two ways, either by summing all "CH_3" products (reaction (43)) or by summing all "Me_3Si" products (reaction (44)). In both cases Φ(8) is missing, an evaluation of which is given in Sections 4.4.1 and 4.4.3. The quantum yield differences $\Phi(CH_3) - \Phi(8)$ and $\Phi(Me_3Si) - \Phi(8)$ agree quite well and there is no discernible dependence on wavelength. It is worthwhile pointing out that the quantum yield for the primary process (I) is wavelength independent at least down to 147 nm [1]. Also the

quantum yield for primary process (II) does not seem to change provided that the formation of Me_2Si (Section 1) is a true primary process and does not result from the decomposition of a vibrationally excited Me_3Si radical.

4.4. Me_4Si photolysis in the presence of additives

In a complex reaction mechanism, the number of reactions occurring is usually much larger than the number of products formed. One way of elucidating the mechanism is to add substances which react in a known manner with one or more of the reactants.

4.4.1. MeOH

It is well known that MeOH reacts with Me_2SiCH_2 to form Me_3SiOMe [27]

$$Me_2SiCH_2 + MeOH \longrightarrow Me_3SiOMe \quad (45)$$

This reaction must be relatively fast because, under the conditions of Fig. 12, an initial concentration of MeOH of about 2×10^{15} cm^{-3} is sufficient to suppress all molecules with Me_2SiCH_2 as a precursor. This is only about a factor of two higher than the total number of Me_2SiCH_2 molecules n formed in the photolysis time t

$$n = I_{abs} t \Phi(Me_2SiCH_2) = 4.9\times10^{15}(0.18)$$
$$= 9\times10^{14} \text{ cm}^{-3}$$

If the initial MeOH concentration drops below the total Me_2SiCH_2 yield, Me_2SiCH_2 will also react with the trimethylsilylmethylether by insertion into the Si–O bond [28]

$$Me_2SiCH_2 + Me_3SiOMe \longrightarrow Me_3SiCH_2SiMe_2OMe \quad (46)$$

At the MeOH concentration at which "Me_2SiCH_2" products have completely disappeared, Me_3SiOMe reaches its plateau value (Fig. 7): $\Phi(Me_3SiOMe) = 0.18\pm0.01$. This value agrees very well with that for $\Phi(Me_2SiCH_2)$ derived in Section 4.3 and shown in Table 2.

A similar dependence on MeOH concentration is shown for Me_6Si_2 and Me_3SiOMe (Fig. 12). The increase in the Me_6Si_2 quantum yield is caused by a release of Me_3Si radicals due to the scavenging of Me_2SiCH_2. Under such circumstances, CH_3 and Me_3Si radicals undergo only combination reactions (disproportionation reactions are disregarded) and a 1 : 1 ratio for $[Me_6Si_2] : [C_2H_6]$ is expected. This is not completely borne out by experiment but very nearly; thus it is assumed that

$$\Phi(Me_6Si_2/MeOH) = \Phi(C_2H_6/MeOH) = 0.11\pm0.01$$

In the case of Me_2SiCH_2 scavenging by MeOH, both Me_3Si and CH_3 radicals are released which brings up the question of why C_2H_6 is unaffected by the addition of MeOH. To understand this, we assume that Me_3Si and CH_3 radicals undergo only reactions (6), (7) and (8) in the presence of MeOH and that $k(8) = 2[k(6)k(7)]^{1/2}$. In this case the following quantum yield ratios should be obtained

$$\Phi(C_2H_6/MeOH) : \Phi(Me_4Si/MeOH) : \Phi(Me_6Si_2/MeOH)$$
$$= 0.11 : 0.22 : 0.11 \quad (47)$$

In the absence of MeOH, fractions of Me_3Si and CH_3 equal to the released radical yield are not available for combination reactions. These fractions are given by

$$\Delta\Phi(Me_3Si) = 2\Phi(Me_3SiSiMe_2CH_2SiMe_3) + \Phi(Me_3SiSiMe_2Et) + \Phi(Me_3SiCH_2SiMe_3) - \Phi(Me_3SiCH_2SiMe_3/MeOH) = 0.09$$

$$\Delta\Phi(CH_3) = 2[\Phi(Me_3SiEt) - \Phi(Me_3SiEt/MeOH)] + \Phi(Me_3SiSiMe_2Et) + \Phi(Me_3SiCH_2SiMe_3) - \Phi(Me_3SiCH_2SiMe_3/MeOH) = 0.05$$

It is evident that Me_3Si and CH_3 radicals react quite differently with Me_2SiCH_2. This may be taken into account by imagining that the rates of formation of the two radicals are different. In such a case the combination product ratio is given by $[C_2H_6] : [Me_4Si] : [Me_6Si_2] = n^2 : 2n : 1$ where the ratio of the rates of formation of CH_3 and Me_3Si is given by n. The ratio has been determined experimentally

$$\frac{\Phi(C_2H_6)}{\Phi(Me_6Si_2)} = \frac{0.108}{0.057} = n^2$$

With $n = 1.376$

$$\Phi(C_2H_6) : \Phi(Me_4Si) : \Phi(Me_6Si_2) = 0.108 : 0.157 : 0.057 \quad (48)$$

$\Delta\Phi(CH_3)$ and $\Delta\Phi(Me_3Si)$ may be calculated

$$\Delta\Phi(Me_3Si) = 2[\Phi(Me_6Si_2/MeOH) - \Phi(Me_6Si_2)] + \Phi(Me_4Si/MeOH) - \Phi(Me_4Si) = 0.168$$

$$\Delta\Phi(CH_3) = 2[\Phi(C_2H_6/MeOH) - \Phi(C_2H_6)] + \Phi(Me_4Si/MeOH) - \Phi(Me_4Si) = 0.067$$

If we compare the product quantum yields in the presence (relationship (47)) and absence (relationship

(48)) of MeOH, it is seen that almost all released CH_3 radicals are used in the formation of Me_4Si, while more than 60% of the Me_3Si radicals form Me_6Si_2 (the rest form Me_4Si). The quality of this model, essentially the geometric mean assumption for $k(8)$, can be tested by a comparison of the calculated and experimental $\Delta\Phi$ values for Me_3Si and CH_3. For CH_3, the agreement is quite satisfactory, but for Me_3Si, the experimental value, $\Delta\Phi(Me_3Si) = 0.09$, is obviously too small. This value accounts only for the increase in Me_6Si_2

$$\Delta\Phi(Me_6Si_2) = \Phi(Me_6Si_2/MeOH) - \Phi(Me_6Si_2) = 0.04$$

It must be concluded that $\Phi(Me_3Si) \approx 0.08$ is hidden in undetected products, which agrees with the findings in Section 4.3 and Table 2.

The substantially different behaviour of some of the products as a function of MeOH concentration at 185 nm can be explained by the direct photolysis of MeOH [29]. The extinction coefficient of MeOH at 185 nm is 213 ± 12 M^{-1} cm^{-1}; the quantum yield for H atom formation is 0.86 ± 0.10. This means that, at the highest MeOH concentration, H atoms should be generated with a quantum yield of about 2.5×10^{-2}

$$MeOH + h\nu \longrightarrow MeO + H \quad (49)$$

This is in reasonable agreement with the H_2 quantum yield measured by mass spectrometry in the presence of MeOH. An increase in $\Phi(Me_3SiH)$ is found, which is attributed to reaction (30). As has already been mentioned, H_2 formation has been observed, and it should be accompanied by Me_3SiCH_2 formation (reaction (29)). If the fate of this radical is described correctly by reactions (3) and (4), the quantum yields of Me_3SiEt and $Me_3SiCH_2SiMe_3$ should increase with increasing MeOH concentration at high MeOH concentration, which is the case (Fig. 7). If

$$\Phi(H_2) = \Phi(Me_3SiCH_2) = \Delta\Phi(Me_3SiEt) + \Delta\Phi(Me_3SiCH_2SiMe_3)$$

where $\Delta\Phi(Me_3SiEt)$ is the difference between the Me_3SiEt quantum yield in the presence of MeOH and the plateau value given in Table 1 and similarly for $\Delta\Phi(Me_3SiCH_2SiMe_3)$, it is concluded that reactions (29) and (30) are about equally important.

The MeO radical can react with the two most abundant radicals, CH_3 and Me_3Si

$$MeO + CH_3 \longrightarrow MeOMe \quad (50)$$

$$MeO + Me_3Si \longrightarrow Me_3SiOMe \quad (51)$$

Dimethylether was not observed, which suggests that the vibrationally excited MeOMe molecule cannot be stabilized under the conditions of these experiments and decomposes to the reactants. This explanation supports the observation that "Me" products such as C_2H_6 are not affected by the presence of MeOH. The main route of formation of Me_3SiOMe is by reaction (45). However, in Fig. 7, there is also a slight increase discernible at higher [MeOH] which is attributed to reaction (51). The quantum yield, $\Phi(Me_3SiSiMe_3)$, goes through a maximum as a function of MeOH concentration. The increase has the same cause as discussed above for 175 nm photolysis, the decrease being caused by a loss of Me_3Si radicals through reactions (30) and (51).

4.4.2. NO

Radicals present in the system were scavenged using NO; however, NO also reacts with Me_2SiCH_2 very effectively

$$Me_2SiCH_2 + NO \longrightarrow \text{products} \quad (52)$$

From the graphs in Fig. 11, in particular by comparing the quantum yields of C_2H_6, Me_6Si_2 and DSCB as a function of NO, we can estimate that the rate constant for reaction (52) is about an order of magnitude larger than for

$$CH_3 + NO + M \longrightarrow CH_3NO + M \quad (53)$$

Under the conditions of this study, this reaction lies deep in the fall off region, $k(53) \approx 2 \times 10^{-12}$ cm^3 s^{-1} [30]. The rate constant for Me_3Si

$$Me_3Si + NO \longrightarrow Me_3SiNO \quad (54)$$

should lie somewhere between these two values. A recently determined value gives $k(54) = 3.3 \times 10^{-11}$ cm^3 s^{-1} [31]. The very large rate constant for reaction (52) leads to a very fast decrease in the quantum yields of those products which originate from Me_2SiCH_2. These are the same molecules already elucidated using MeOH. Furthermore, by using NO it can be seen that both Me_3SiEt and $Me_3SiCH_2SiMe_3$ are formed by more than one process. The maximum in the $\Phi(Me_3SiEt)$ vs. [NO] curve may be related to the quenching of reaction (14) while reaction (13) is only slightly affected by NO. The quantum yields $\Phi(C_2H_6)$ and $\Phi(Me_3SiH)$ also go through a maximum. This is easily understood for C_2H_6; the much faster scavenging rate for Me_3Si leaves more CH_3 radicals to react via reaction (6). The reason for the maximum for $\Phi(Me_3SiH)$ is not understood, but is probably connected with the unknown reactions following reaction (54). The behaviour of Me_2HSiEt and $Me_2HSiCH_2SiMe_3$ supports the assessment made in Section 4.2 that the two products are not formed via Me_2SiCH_2.

4.4.3. GeH_4

The addition of GeH_4 influences both Me_3Si and CH_3 radicals, but leaves DSCB essentially unaffected. As can be seen from Fig. 8, Me_3Si radicals react quite clearly with GeH_4 by H atom abstraction

$$Me_3Si + GeH_4 \longrightarrow Me_3SiH + GeH_3 \quad (55)$$

There is also a slight decrease in $\Phi(C_2H_6)$ and an increase in $\Phi(CH_4)$; this could be due to an abstraction reaction

$$CH_3 + GeH_4 \longrightarrow CH_4 + GeH_3 \quad (56)$$

or to a disproportionation reaction with the GeH_3 radicals formed in reaction (55)

$$CH_3 + GeH_3 \longrightarrow CH_4 + GeH_2 \quad (57)$$

The quantum yield of Me_3SiH formation in reaction (55), $\Delta\Phi(Me_3SiH/GeH_4) \approx 0.27$, is much larger than the decrease in the Me_3Si quantum yield

$$\begin{aligned}\Delta\Phi(Me_3Si) = {} & 2\Delta\Phi(Me_6Si_2) + \Delta\Phi(Me_3SiCH_2SiMe_2H) \\ & + \Delta\Phi(Me_3SiCH_2SiMe_3) \\ & + \Delta\Phi(Me_3SiSiMe_2Et) \\ & + 2\Delta\Phi(Me_3SiSiMe_2CH_2SiMe_3) \\ = {} & 0.17\end{aligned}$$

This is a clear indication that the Me_3Si radical is involved in a hidden reaction which is associated with reaction (8). The addition of GeH_4 elicits different responses from Me_2HSiEt and $Me_2HSiCH_2SiMe_3$. The two substances are thought to be formed via the reaction sequences (39), (34) and (39), (33) respectively. Reaction (33) should be suppressed by reaction (55); therefore a decrease in $Me_2HSiCH_2SiMe_3$ is expected, as was observed. However, Me_2HSiEt increases, which means that a new path has been opened for its formation. This must either be due to an abstraction reaction of an Me_2EtSi radical from GeH_4 or a disproportionation reaction with GeH_3

$$Me_2EtSi + GeH_4 \longrightarrow Me_2HSiEt + GeH_3 \quad (58)$$

The Me_2SiEt and Me_3SiCH_2 radicals are formed through reaction (10). If it is assumed that, at the highest GeH_4 concentration, most of the silicon-centred radicals react by abstraction while the carbon-centred radicals are only slightly affected, we obtain

$$\Delta\Phi(Me_2HSiEt/GeH_4) = 2.7 \times 10^{-3} \approx \Phi(10b)$$

$$CH_3 + Me_2SiCH_2 \longrightarrow Me_3SiCH_2 \quad (10a)$$

$$CH_3 + Me_2SiCH_2 \longrightarrow Me_2SiEt \quad (10b)$$

and $\Phi(10b)$ is about 33% of reaction (10)

$$\Phi(10) = \Phi(Me_3SiEt/MeOH) = 8 \times 10^{-3}$$

This means that the addition of CH_3 is more likely to occur on the Si side of the Si=C double bond than on the C side.

The quenching experiments with GeH_4 allow an assertion to be made about the quantum yield of primary process (II). If all the reactions of the Me_3Si radical are condensed in our system in the following three equations

$$Me_4Si + h\nu \longrightarrow Me_3Si + CH_3 \quad (II)$$

$$Me_3Si + R \longrightarrow \text{products} \quad (59)$$

$$Me_3Si + GeH_4 \longrightarrow Me_3SiH + GeH_3 \quad (60)$$

where R stands for the radicals present in the system and $k(59)$ is the weighted mean rate constant, the following equation is obtained

$$\frac{1}{\Phi(Me_3SiH)} = \frac{k(59)[R]}{k(55)\Phi(II)} \frac{1}{[GeH_4]} + \frac{1}{\Phi(II)}$$

As can be seen from Fig. 16, a straight line results with a slope

$$\frac{k(59)[R]}{k(55)\Phi(II)} = 7 \times 10^{14}\ cm^{-3}$$

and an intercept

$$1/\Phi(II) = 2.28 \pm 0.06$$

$$\Phi(II) = \Phi(Me_3Si) = 0.44 \pm 0.01$$

This value is rather close to that estimated using the geometric mean rule. In Section 4.3, a value for $\Phi(Me_3Si) - \Phi(8) = 0.254$ was derived (Table 2) and, in Section 4.4.1, a value for $\Phi(8) = 0.157$ was also derived, giving $\Phi(II) = 0.41$. A value of $\Phi(II) = 0.45 \pm 0.05$ for the quantum yield of primary process (II) is suggested.

4.4.4. SF_6

The influence of SF_6 on the product quantum yields was caused to a great extent by its water impurity. Almost all products decrease with increasing SF_6 pres-

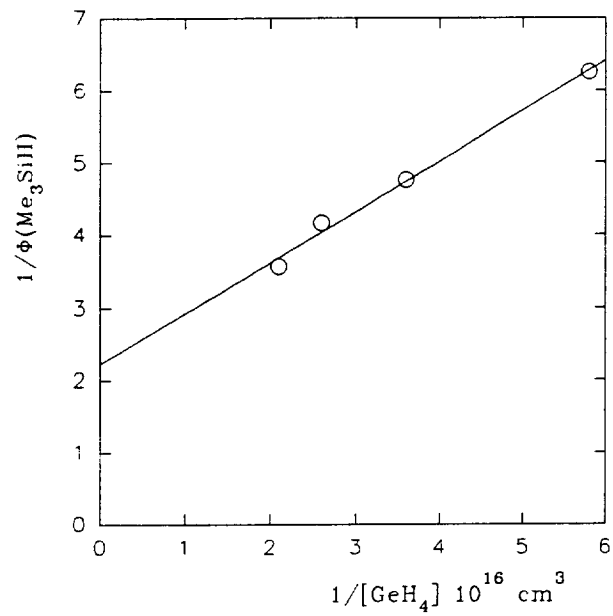

Fig. 16. Determination of $\Phi(II)$ from a plot of $1/\Phi(Me_3SiH)$ vs. $1/[GeH_4]$.

sure and this was attributed to the rapid reaction

$$Me_2SiCH_2 + H_2O \longrightarrow Me_3SiOH \quad (61)$$

Only two products, Me_2HSiEt and $Me_2HSiCH_2SiMe_3$, show a more pronounced dependence and this could be due to the deactivation of hot Me_3Si radicals

$$Me_3Si^{v} + SF_6 \longrightarrow Me_3Si + SF_6 \quad (62)$$

The reason for the decrease in Me_6Si_2 is less clear, but in part is caused by

$$Me_3Si + SF_6 \longrightarrow Me_3SiF + SF_5 \quad (63)$$

A similar reaction of dimethylchlorosilyl radical has been reported by Davidson and Dean [32]. On the other hand, Me_3SiH shows only a very slight dependence, which is thought to be due in part to disproportionation reactions of hot Me_3Si radicals.

4.5. Relative rate constants

A number of relative rate constants can be determined from the assumed reaction mechanism (Table 2) and the quantum yields given in Table 1. From Eqs. (6), (7) and (8), the cross-combination rate constant is calculated

$$\frac{k(8)}{\sqrt{k(6)k(7)}} = \frac{\Phi(Me_4Si)}{\sqrt{\Phi(C_2H_6)\Phi(Me_6Si_2)}} = 2.7 \pm 0.8$$

Similar rate constant ratios can be obtained for the reaction of CH_3 and Me_3Si radicals with Me_2SiCH_2. Before this may be done, the relative importance of CH_3 and Me_3Si attack on Me_2SiCH_2 must be calculated. To do this, the mechanism is simplified by assuming the same rate constant for all radical–radical reactions (12)–(19). However, distinction is made between radical addition to the silicon centre, $k(10a)$ and $k(11a)$, and to the carbon centre, $k(10b)$ and $k(11b)$, of the Si=C double bond. The following equations are derived

$$\Phi(Me_3SiEt) - \Phi(Me_3SiEt/MeOH) = \frac{[k(10a)+k(10b)][CH_3][Me_2SiCH_2]}{I_{abs}} \times \frac{[CH_3]}{[CH_3]+[Me_3Si]} = 8\times10^{-3}$$

$$\Phi(Me_3SiCH_2SiMe_3) - \Phi(Me_3SiCH_2SiMe_3/MeOH) = \frac{k(10a)[CH_3][Me_2SiCH_2]}{I_{abs}} \times \frac{[Me_3Si]}{[CH_3]+[Me_3Si]} + \frac{k(11b)[Me_3Si][Me_2SiCH_2]}{I_{abs}} \frac{[CH_3]}{[CH_3]+[Me_3Si]} = 8\times10^{-3}$$

$$\Phi(Me_3SiSiMe_2Et) = \frac{k(10b)[CH_3][Me_2SiCH_2]}{I_{abs}} \frac{[Me_3Si]}{[CH_3]+[Me_3Si]} + \frac{k(11a)[Me_3Si][Me_2SiCH_2]}{I_{abs}} \frac{[CH_3]}{[CH_3]+[Me_3Si]} = 3.3\times10^{-2}$$

$$\Phi(Me_3SiSiMe_2CH_2SiMe_3) = \frac{[k(11a)+k(11b)][Me_3Si][Me_2SiCH_2]}{I_{abs}} \times \frac{[Me_3Si]}{[CH_3]+[Me_3Si]} = 3.6\times10^{-2}$$

These equations allow two solutions for the mole fractions of CH_3 and Me_3Si

$$\frac{[CH_3]}{[CH_3]+[Me_3Si]} = 0.472,\ 0.200$$

The relative stationary concentration of CH_3 and Me_3Si is determined mainly by reactions (6), (7) and (8). The rate constants for these processes are quite similar, and therefore 0.472 is adopted as the value for this system. Using this value we obtain

$$[k(10a)+k(10b)]\frac{[CH_3][Me_2SiCH_2]}{I_{abs}} = 0.017$$

$$[k(11a)+k(11b)]\frac{[Me_3Si][Me_2SiCH_2]}{I_{abs}} = 0.068$$

and finally the ratio $k(10)/k(11)$

$$\frac{k(10a)+k(10b)}{k(11a)+k(11b)} = \frac{k(10)}{k(11)} = \frac{0.017}{0.068}\frac{[Me_3Si]}{[CH_3]} = \frac{(0.017)(0.528)}{(0.068)(0.472)} = 0.28$$

Trimethylsilyl radicals are much faster than methyl radicals in adding to the Si=C double bond, in agreement with the results in Section 4.4.1. To obtain an upper limit for $k(11b)/k(11a)$, it is assumed that CH_3 radicals add exclusively to the carbon end of the Si=C double bond, making $k(10a)=0$

$$\frac{k(11b)}{k(11a)} \leqslant 0.33$$

However, in Section 4.4.3 it was estimated that

$$\frac{k(10b)}{k(10a)+k(10b)} = 0.33$$

Using this value

$$\frac{k(11b)}{k(11a)} = 0.07$$

This analysis indicates that Me_3Si radicals add almost exclusively to the Si end of the Si=C double bond, in agreement with theory [33]. It is now possible to calculate

$$\frac{k(10)}{\sqrt{k(6)k(9)}} = \frac{\Phi(P_C)}{\sqrt{\Phi(C_2H_6)\Phi(DSCB)}}$$

and

$$\frac{k(11)}{\sqrt{k(7)k(9)}} = \frac{\Phi(P_{Si})}{\sqrt{\Phi(Me_6Si_2)\Phi(DSCB)}}$$

where P_C represents all products formed by reaction (10) followed by reactions (12), (13), (14) and (16) and P_{Si} represents all products formed by reactions (11), (15), (17), (18) and (19); $\Phi(P_C)$ and $\Phi(P_{Si})$ are given by

$$\Phi(P_C) = \Phi(Me_3SiEt) - \Phi(Me_3SiEt/MeOH) + \frac{k(10a)}{k(10a)+k(11b)}[\Phi(Me_3SiCH_2SiMe_3) - \Phi(Me_3SiCH_2SiMe_3/MeOH)] + \frac{k(10b)}{k(10b)+k(11a)}\Phi(Me_3SiSiMe_2Et)$$

$$\Phi(P_C) = 0.01 - 0.002 + 0.73(0.0094 - 0.0014) + (0.091)(0.033) = 0.0168$$

$$\Phi(P_{Si}) = \frac{k(11b)}{k(10a)+k(11b)}[\Phi(Me_3SiCH_2SiMe_3) - \Phi(Me_3SiCH_2SiMe_3/MeOH)] + \frac{k(11a)}{k(10b)+k(11a)}\Phi(Me_3SiSiMe_2Et) + \Phi(Me_3SiSiMe_2CH_2SiMe_3)$$

$$\Phi(P_{Si}) = (0.27)(0.008) + (0.909)(0.033) + 0.036 = 0.0658$$

$$\frac{k(10)}{\sqrt{k(6)k(9)}} = 0.30$$

$$\frac{k(11)}{\sqrt{k(7)k(9)}} = 1.7$$

For $k(6)$, $k(7)$ and $k(9)$, there exist absolute rate constants which allow the calculation of the absolute values for $k(10)$ and $k(11)$ (see Section 4.6). From the last two rate constant ratios, it is possible to calculate $k(7)$ relative to $k(6)$ because the ratio $k(10)/k(11)$ has already been determined.

$$\sqrt{\frac{k(7)}{k(6)}} = \frac{0.30}{1.7}\frac{k(12)}{k(11)} = 0.18(3.57) = 0.63$$

$$\frac{k(7)}{k(6)} = 0.4$$

compared with a literature value of 0.67 [17,34].

The reactions of Me_2SiCH_2 with MeOH and NO are so rapid that appropriate experimental conditions, particularly the constancy of the scavenger concentration, could not be established. Therefore it is not possible to extract a relative rate constant for reactions (45) and (52) in the usual manner and computer simulations must be relied upon (see Section 4.6).

The experiments with GeH_4 allow the determination of the rate constant for reaction (60), the hydrogen abstraction of Me_3Si from GeH_4. The following relationship should apply

$$\frac{\Phi(Me_3SiH)}{\sqrt{\Phi(Me_6Si_2)}} = \frac{\Phi_0(Me_3SiH)}{\sqrt{\Phi_0(Me_6Si_2)}} + \frac{k(60)}{\sqrt{k(7)}}\frac{[GeH_4]}{\sqrt{I_{abs}}}$$

From the slope of Fig. 17

$$\frac{k(60)}{\sqrt{k(7)}} = 5.3\times10^{-9}\ cm^{3/2}\ s^{-1/2}$$

This value is an upper limit because some of the Me_3SiH could also be formed by

$$Me_3Si + GeH_3 \longrightarrow Me_3SiH + GeH_2 \quad (64)$$

The large intercept in Fig. 17 is not accounted for by the mechanism. If it is assumed that the CH_3 radicals also undergo abstraction reaction (56), a relative rate constant

$$\frac{k(56)}{\sqrt{k(6)}} = 6.5\times10^{-10}\ cm^{3/2}\ s^{-1/2}$$

is derived which has the expected intercept. Perhaps this is an indication that, in the case of Me_3Si radicals, vibrational excitation plays some role.

4.6. Computer simulations

Computer simulations [35] allow a more stringent test of the assumed mechanism than the semiquantitative considerations made so far. The mechanism with the pertinent rate constants is given in Table 3. The two major decomposition channels have been taken into account with a quantum yield of 0.2 for the CH_4 elimination (channel (I)) and a quantum yield of 0.5 for channel (II). The rate constant for reaction (6) is well known [36]; for $k(7)$ there are only two literature values, both of low precision [17,34]. The quantum

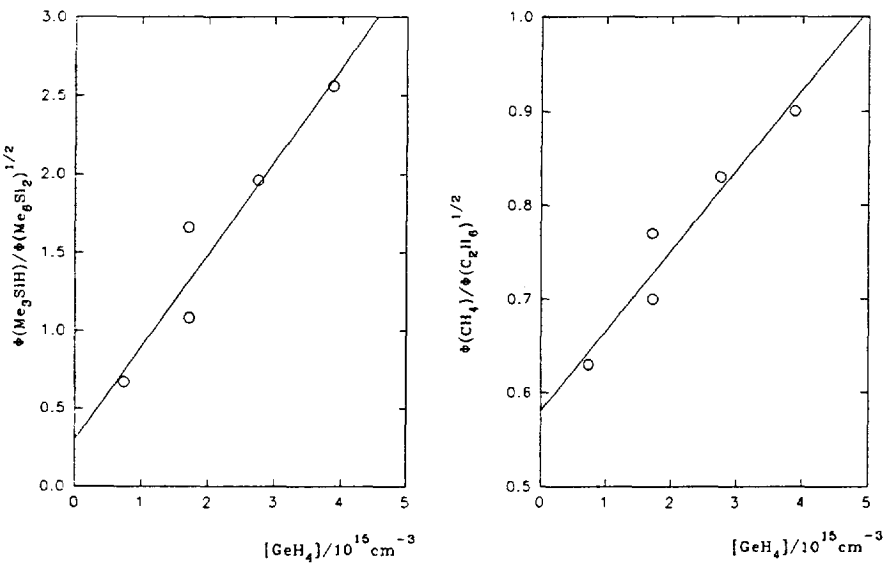

Fig. 17. Determination of the relative rate constants $k(60)/k(7)^{1/2}$ and $k(56)/k(6)^{1/2}$ from plots of $\Phi(Me_3SiH)/\Phi(Me_6Si_2)^{1/2}$ and $\Phi(CH_4)/\Phi(C_2H_6)^{1/2}$ vs. $[GeH_4]$ ($I_{abs}=1.1\times10^{14}$ cm^{-3} s^{-1}).

yields of C_2H_6 and Me_6Si_2 are sensitive to $k(8)$ as well as $k(6)$ and $k(7)$ and a good fit is obtained for a rate constant ratio of

$$\frac{k(8)}{\sqrt{k(6)k(7)}}=2.4$$

The value for $k(9)$ has been taken from the literature [12]. No absolute rate constants are known for the radical addition to the Si=C double bond. The rate constant ratio

$$\frac{k(11)}{\sqrt{k(9)k(7)}}=1.7$$

for Me_3Si found in the simulation agrees with the analysis in Section 4.5; the corresponding ratio for CH_3 is 0.69; this is larger by a factor of two than anticipated in Section 4.5. The preference for Me_3Si radical addition to the Si centre is seen clearly from the rate constant ratio

$$\frac{k(11a)}{k(11b)}=14$$

and cannot be crucially changed by assuming different rate constants for the radical combination reactions (12)–(19). This statement does not necessarily apply to the CH_3 radical addition; other rate constant ratios may describe the product distribution equally well.

The mechanism in this study is an oversimplification with respect to reaction (39); therefore no direct physical meaning can be assigned to the value of $k(39)$. A more appropriate mechanism might be

$$Me_4Si+h\nu \longrightarrow Me_3Si^{v}+CH_3 \qquad \Phi(II)I_{abs}$$

$$Me_3Si^{v} \longleftrightarrow Me_2HSiCH_2^{v} \qquad (39,-39)$$

$$Me_2HSiCH_2^{v}+M \longrightarrow Me_2HSiCH_2+M \qquad (40)$$

$$Me_3Si^{v}+M \longrightarrow Me_3Si+M \qquad (65)$$

From these reactions

$$\Phi(Me_2HSiCH_2) = \frac{k(40)}{k(65)}+\frac{k(39)}{k(-39)+k(40)[M]}\Phi(Me_3Si) \approx \frac{k(39)}{k(-39)+k(40)[M]}\Phi(Me_3Si)$$

This expression may explain the slight pressure dependence of $\Phi(Me_2HSiEt)$ and $\Phi(Me_2HSiCH_2SiMe_3)$ with respect to SF_6 and their wavelength dependence.

The loss of Me_2SiCH_2, mentioned in Section 4.3, cannot be accounted for by simple diffusion to the wall. In the investigation of the photochemistry of $Me_3SiCH_2CH_2CH_2$, it was found that a bimolecular step also leads to irretrievable products [12].

The results of the computer calculations show that the stationary radical concentrations of CH_3 and Me_3Si are almost the same, while the concentrations of all other radicals are at least one order of magnitude smaller, with the exception of the concentration of $Me_3SiSiMe_2CH_2$, which is rather large. The computer simulation therefore predicts $(Me_3SiSiMe_2CH_2)_2$ as a product with a quantum yield of 3.5×10^{-3}. This product was not observed; otherwise the agreement with the experimental quantum yields is satisfactory.

To simulate the results in the presence of MeOH at 175 nm, only two reactions, (45) and (46), need to be added to the mechanism. In Fig. 18, the experiments are compared with computer simulations for different values of the rate constant $k(45)$. The value 3×10^{-14} cm^3 s^{-1} for this rate constant is quite clearly too small,

Table 3
Mechanism and rate constants used in the computer simulations

Reaction number	Reaction	Φ
(I)	$Me_4Si \rightarrow CH_4 + Me_2SiCH_2$	0.2
(II)	$Me_4Si \rightarrow CH_3 + Me_3Si$	0.5
Reaction number	**Reaction**	**k (10^{-11} cm^3 s^{-1})**
(6)	$2CH_3 \rightarrow C_2H_6$	4.5
(7)	$2Me_3Si \rightarrow Me_6Si_2$	3.0
(8)	$Me_3Si + CH_3 \rightarrow Me_4Si$	9.0
(9)	$2Me_2SiCH_2 \rightarrow$ DSCB	3.0
(10b)	$CH_3 + Me_2SiCH_2 \rightarrow Me_2SiEt$	0.48
(10a)	$CH_3 + Me_2SiCH_2 \rightarrow Me_3SiCH_2$	0.95
(11b)	$Me_3Si + Me_2SiCH_2 \rightarrow Me_3SiCH_2SiMe_2$	0.33
(11a)	$Me_3Si + Me_2SiCH_2 \rightarrow Me_3SiSiMe_2CH_2$	4.8
(12)	$CH_3 + Me_3SiCH_2 \rightarrow Me_3SiEt$	4.0
(13)	$CH_3 + Me_2SiEt \rightarrow Me_3SiEt$	4.0
(14)	$Me_3Si + Me_3SiCH_2 \rightarrow Me_3SiCH_2SiMe_3$	5.0
(15)	$CH_3 + Me_3SiCH_2SiMe_2 \rightarrow Me_3SiCH_2SiMe_3$	4.0
(16)	$Me_3Si + Me_2SiEt \rightarrow Me_3SiSiMe_2Et$	3.3
(17)	$CH_3 + Me_3SiSiMe_2CH_2 \rightarrow Me_3SiSiMe_2Et$	3.0
(18)	$Me_3Si + Me_3SiSiMe_2CH_2 \rightarrow Me_3SiSiMe_2CH_2SiMe_3$	4.0
(19)	$Me_3Si + Me_3SiCH_2SiMe_2 \rightarrow Me_3SiSiMe_2CH_2SiMe_3$	3.3
(20)	$2Me_3Si \rightarrow Me_3SiH + Me_2SiCH_2$	0.6
(33)	$Me_3Si + Me_2HSiCH_2 \rightarrow MeHSiCH_2SiMe_3$	4.0
(34)	$CH_3 + Me_2HSiCH_2 \rightarrow Me_2HSiEt$	3.3
	$2Me_2SiCH_2 \rightarrow P$	2.0
(39)	$Me_3Si \rightarrow Me_2HSiCH_2$	0.23 s^{-1}
	$Me_3Si \rightarrow Me_3Si_w$	1.0 s^{-1}
(45)	$Me_2SiCH_2 + MeOH \rightarrow Me_3SiOCH_3$	$\geqslant 0.03$
(46)	$Me_2SiCH_2 + Me_3SiOCH_3 \rightarrow Me_3SiCH_2SiMe_2OCH_3$	2×10^{-4}
(68)	$Me_2SiCH_2 + NO \rightarrow P$	1.0
(66)	$CH_3 + NO \rightarrow CH_3NO$	0.1
(67)	$Me_3Si + NO \rightarrow P$	3.3
	$Me_2HSiCH_2 + NO \rightarrow P$	1.0
(69)	$Me_3Si + P \rightarrow P$	0.002
(70)	$Me_2SiCH_2 + P \rightarrow P$	0.008
(56)	$CH_3 + GeH_4 \rightarrow CH_4 + GeH_3$	5×10^{-4}
(55)	$Me_3Si + GeH_4 \rightarrow Me_3SiH + GeH_3$	4×10^{-3}
(58)	$Me_2SiEt + GeH_4 \rightarrow Me_2HSiEt + GeH_3$	2×10^{-3}
	$Me_3SiCH_2SiMe_2 + GeH_4 \rightarrow Me_2HSiCH_2SiMe_3 + GeH_3$	1×10^{-3}
	$CH_3 + GeH_3 \rightarrow P$	3.0
	$Me_3Si + GeH_3 \rightarrow P$	3.0
	$Me_2SiEt + GeH_3 \rightarrow P$	3.0
	$Me_2SiCH_2 + GeH_3 \rightarrow P$	3.0
	$Me_3SiCH_2 + GeH_3 \rightarrow P$	3.0
	$Me_3SiSiMe_2CH_2 + GeH_3 \rightarrow P$	3.0
	$Me_3SiCH_2SiMe_2 + GeH_3 \rightarrow P$	3.0
	$2GeH_3 \rightarrow P$	3.0

but for the other two values similar results were obtained. The differences lie within experimental error and only a lower limit for $k(45)$ was determined: $k(45) \geqslant 3\times10^{-13}$ cm^3 s^{-1}.

Reaction (45) is probably not a concerted reaction; nevertheless, an A factor larger than 5×10^{-12} cm^3 s^{-1} for this reaction is not expected. This means that this reaction proceeds with zero, or only a very small, activation energy. The rate constant for Me_2SiCH_2 insertion into the Si–O bond is about two orders of magnitude smaller than insertion into the O–H bond. Thus reaction (46) comes into play only if MeOH has been depleted.

In the presence of NO, a complex mechanism takes place, the individual steps of which are not known. The fact that Me_3Si and Me_2SiCH_2 were found to react

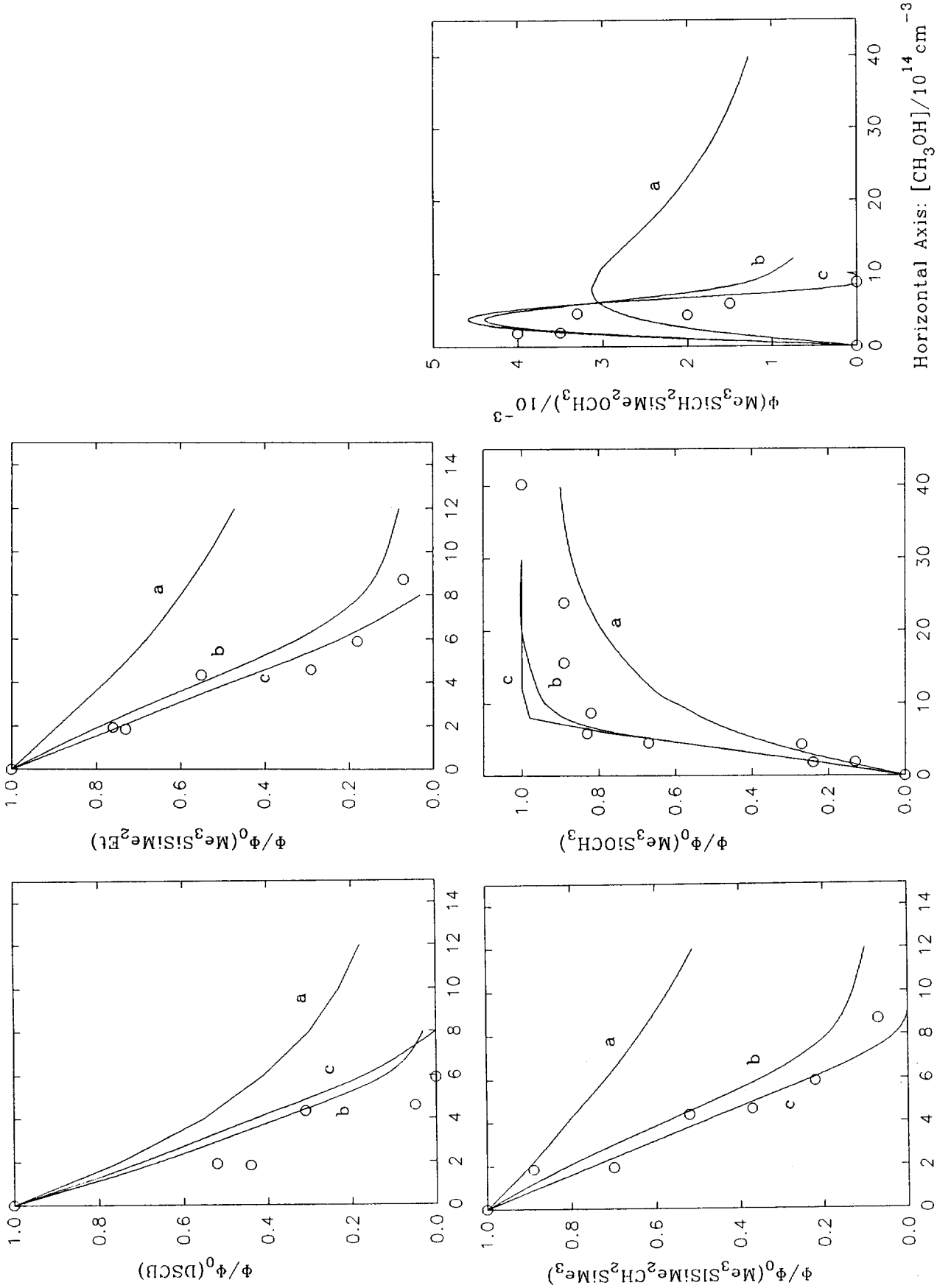

Fig. 18. Computer simulations of the dependence of the relative quantum yields, Φ/Φ_0, of DSCB and $Me_3SiSiMe_2C_2H_5$ and $\Phi(Me_3SiCH_2SiMe_2OCH_3)$ on MeOH concentration for different values of $k(45)$; Φ_0 is the quantum yield in the absence of MeOH: (a) $k(45)=3\times10^{-14}$; (b) $k(45)=3\times10^{-13}$; (c) $k(45)=3\times10^{-12}$.

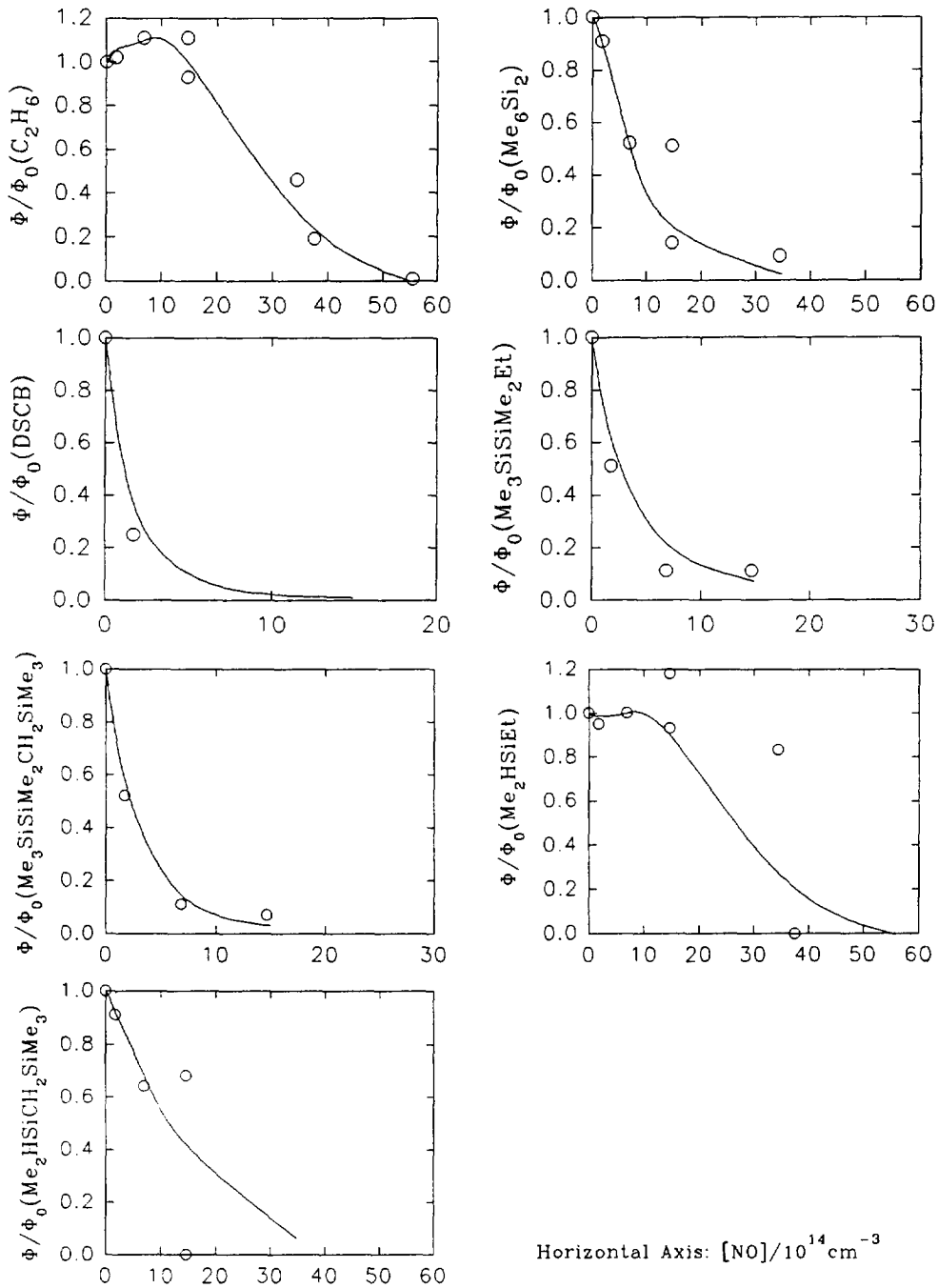

Fig. 19. Computer simulations of the dependence of the relative quantum yields Φ/Φ_0 of various products on NO concentration (Φ_0 is the quantum yield in the absence of NO).

with NO scavenging products has been accounted for in a simplified manner by postulating a single product P

$$CH_3 + NO \longrightarrow CH_3NO \quad (66)$$

$$Me_3Si + NO \longrightarrow P \quad (67)$$

$$Me_2SiCH_2 + NO \longrightarrow P \quad (68)$$

$$Me_3Si + P \longrightarrow P \quad (69)$$

$$Me_2SiCH_2 + P \longrightarrow P \quad (70)$$

This gross simplification prohibits the determination of a value for $k(52)$, but with reasonable estimates for the rate constants $k(68)$–$k(70)$, it is possible to rationalize a large number of experimentally observed phenomena (Fig. 19), i.e. the rapid disappearance of DSCB and all other products which are formed by Me_2SiCH_2, the increase in the C_2H_6 quantum yield at small NO concentrations and, most significantly, the unexpectedly

different behaviour of Me_2HSiEt and $Me_2HSiCH_2SiMe_3$. The satisfactory agreement between experimental and calculated quantum yields for these two products is a further confirmation that they both have the Me_2HSiCH_2 radical as a precursor and that the Me_2HSiCH_2 radical is not formed by H addition to Me_2SiCH_2. The mechanism fails to reproduce the very pronounced maximum in the Me_3SiH quantum yield curve.

In the presence of GeH_4, the mechanism was extended in the following manner

$$R + GeH_4 \longrightarrow RH + GeH_3 \quad (71)$$

$$R + GeH_3 \longrightarrow \text{products} \quad (72)$$

where R is a radical present in the system. The rate constants for reaction (71) depend on the nature of R and are given in Table 3. For radical combination, a rate constant independent of R has been chosen. As can be seen from Fig. 20, the main features of this experiment can be reproduced except for Me_2HSiEt, suggesting a discrepancy in the proposed mechanism for its formation.

4.7. Photophysical processes

The ultimate goal of a photochemical study is an understanding of the primary photochemical processes in terms of the topology of the potential surfaces involved. In the case of Me_4Si, there is only limited knowledge of the ground state potential energy surface in the immediate neighbourhood of the potential minimum and of the energetics of the dissociation channels (I) and (II). It is known, however, that the first band in the absorption spectrum corresponds to the excitation of an electron in the highest occupied molecular orbital (HOMO) to a Rydberg 4s orbital [37].

The electronic structure of Me_4Si, in terms of symmetry adapted orbitals, can be obtained most easily by taking localized Si–C and C–H orbitals as a basis [38]. For T_d symmetry, we obtain: $(1a_1)^2(1t_2)^2(2a_1)^2(2t_2)^6(e)^4(t_1)^6(3t_2)^6\ {}^1A_1$. Theory [39], as well as experiment [38,39], suggests that, energetically, the $3t_2$ orbital, which has predominant Si–C bonding character, is the highest lying occupied orbital. Excitation from this orbital into a non-bonding 4s Rydberg orbital gives rise to a $^1T_2$ excited state. This state should be subject to Jahn–Teller distortion in the same manner as the Me_4Si ion in the $^2T_2$ ground state. In the photoelectron spectrum of Me_4Si, a splitting of the lowest energy band into three subbands is indeed observed [38,39]. Proof for the correct assignment of the excited state has been inferred from the shoulder in the first absorption band which indicates a Jahn–Teller splitting similar to that in the ion [37]. The excited state may be distorted either to D_{2d} symmetry by an E vibration or to C_{3v} symmetry by a T_2 vibration. Because of the weak influence of the Rydberg 4s electron on the core, some similarity between the ground state potential energy surface of the ion and the Rydberg state is expected. In the theory of mass spectra, it is assumed that the first generation fragment ions originate from unimolecular decomposition on the ground state potential energy surface of the ion. In the mass spectrum, we observe a molecular ion peak at *m/e* 88 of very low intensity, a fragment ion at *m/e* 73 which dominates the spectrum and an ion peak of very low intensity at

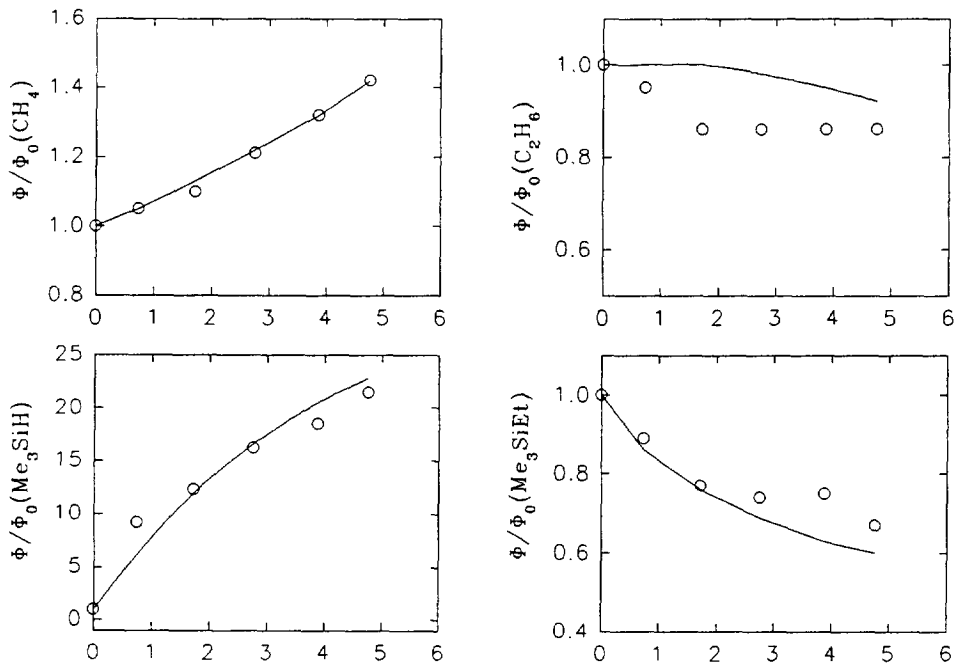

Fig. 20. *(continued)*

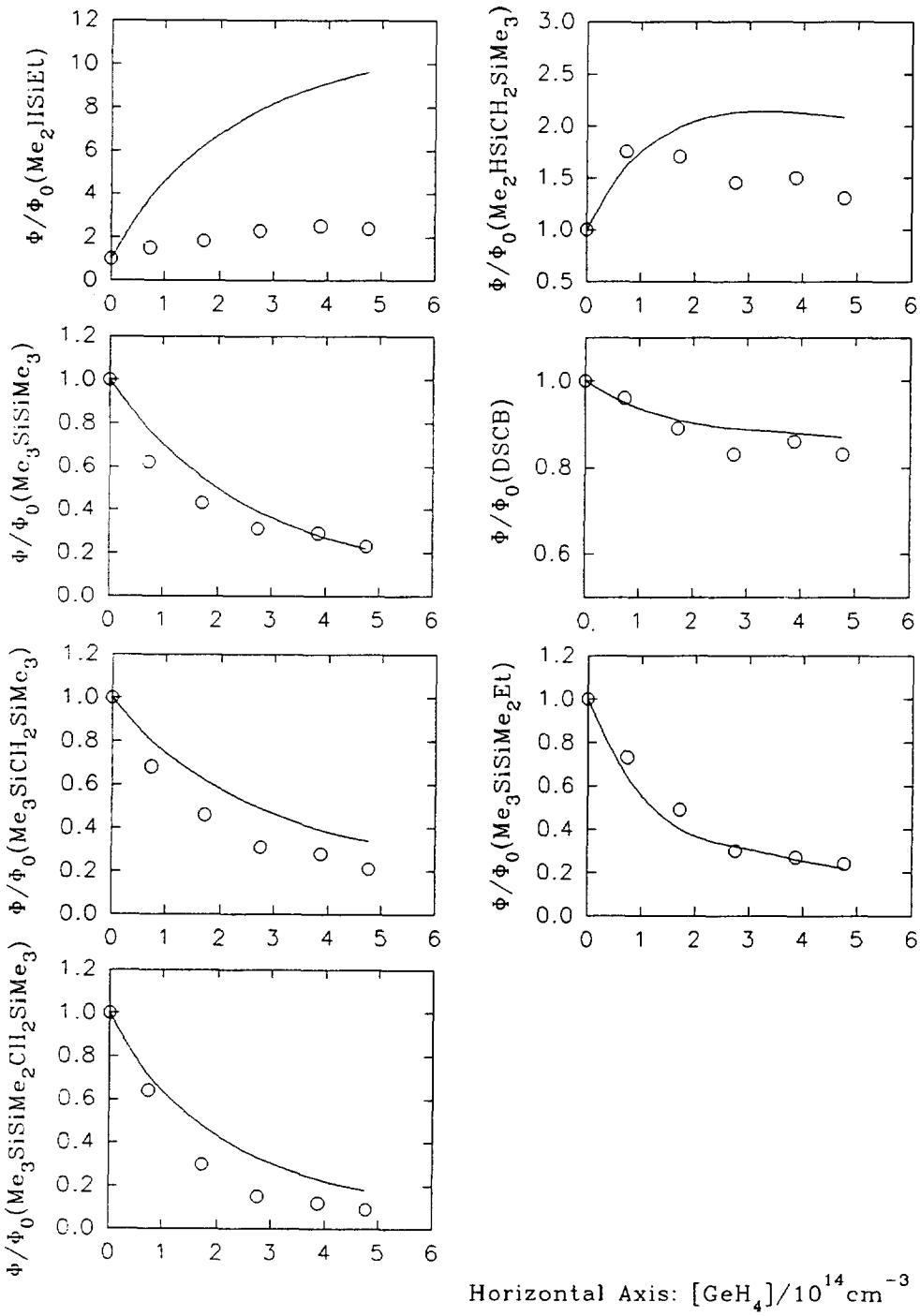

Fig. 20. Computer simulations of the dependence of the relative quantum yields Φ/Φ_0 of various products on GeH_4 concentration (Φ_0 is the quantum yield in the absence of GeH_4).

m/e 72. From these observations, it is concluded that the potential energy surface is stable, and the predominant decomposition process is

$$Me_4Si^+(m/e\ 88) \longrightarrow Me_3Si^+(m/e\ 73) + CH_3 \quad (73)$$

and that methane elimination

$$Me_4Si^+(m/e\ 88) \longrightarrow Me_2SiCH_2{}^+(m/e\ 72) + CH_4 \quad (74)$$

plays virtually no role.

The energetic positions of the two channels (73) and (74) are known; the appearance potentials (AP)

$AP(Me_3Si^+ \longleftarrow Me_4Si) = (10.09 \pm 0.01)$ eV [40]

$AP(Me_2SiCH_2^+ \longleftarrow Me_4Si) = 10.4$ eV

are in agreement with the preference for Si–C bond breaking. In the photoelectron spectrum of Me_4Si, the ionization onset is observed at about 9.8 eV. If this is equated with the adiabatic ionization potential of Me_4Si, the Si–C bond energy in the ion would amount to only 0.3 eV. This very small value is not considered to be real, but is thought to be caused by the Jahn–Teller effect, leading to a large displacement of the equilibrium configuration of the ion. A similar effect is thought to be operating in the case of the Rydberg state, with the absorption onset lying far above the 0–0 transition. For alkanes it has been demonstrated that a large gap exists between the absorption onset at about 160 nm and the fluorescence emission at 207 nm [41]. The 0–0 transition lies somewhere between these two extremes. If a similar situation prevails in the case of Me_4Si, the position of the Jahn–Teller relaxed Rydberg states is expected at about 200–220 nm (approximately 570 kJ mol^{-1}).

Excitation of an electron from a t_2 orbital to a Rydberg 4s orbital also gives rise to a triplet state. The singlet–triplet splitting is small in Rydberg states and can be correlated with the term value of the Rydberg state [37]. For neopentane, whose lowest excited state is a 3s Rydberg state with a term value similar to Me_4Si, the singlet–triplet splitting is 2000 cm^{-1} [37]. This value may increase somewhat if the Jahn–Teller relaxed states possess an enhanced valence character, but in any case the triplet state of Me_4Si will lie quite close in energy to the corresponding singlet state.

The energetic positions of the two major decomposition channels (I) and (II) are quite well known for the ground state potential energy surface. Taking $\Delta H_f(CH_3) = 146$ kJ mol^{-1} [8], $\Delta H_f(Me_3Si) = 17$ kJ mol^{-1} [42] and $\Delta H_f(Me_4Si) = -231$ kJ mol^{-1} [11], $\Delta H(II) = 394$ kJ mol^{-1} is calculated; the reaction enthalpy of channel (I) is $\Delta H(I) = 217$ kJ mol^{-1}. This value was calculated using $\Delta H_f(Me_2SiCH_2) = 61$ kJ mol^{-1}. The latter value has been recalculated from the data in Ref. [12] using a newer value for $\Delta H_f(Me_3SiCH_2CH_2CH_2) = -85$ kJ mol^{-1} [43], bringing experiment and theory [44] into better agreement.

Intuitively, we expect a high activation energy for channel (I) and, in fact, this channel has not been considered either for thermally [45] or chemically [46] activated systems. Concerning the magnitude of the activation energy, we can rely on theoretical calculations for similar systems. Gordon and Truong [47] have shown that 1,2 H_2 elimination from $MeSiH_3$ has a higher activation energy than the Si–C bond breaking process. The activation energy for a 1,2 CH_4 elimination in Me_4Si should be even higher [48]. The activation barrier is shown schematically in Fig. 21.

The energetic positions of channnels (I) and (II) for excited states may be estimated from data available in the literature. The singlet–triplet energy difference $E(T_1) - E(S_0)$ for Me_2SiCH_2 has been calculated to be 150 kJ mol^{-1} [49] and from the absorption spectrum it is estimated that $E(S_1) - E(S_0) = 400$ kJ mol^{-1} [12]. The energetic positions of these two dissociation channels are also shown in Fig. 21. It is probable that additional activation barriers are also operating in the excited states. The lowest Si–C dissociation channel also correlates with the triplet state, implying a repulsive character of the triplet potential energy surface with respect to this decomposition mode. The energetic position of the Si–C dissociation channel correlating with the excited singlet state is calculated, in the same manner, from the absorption spectrum of Me_3Si [17]. The energetic position of this channel lies far above the available photon energies. According to the potential energy diagram, decomposition should not occur from the excited state reached by the absorption process. The two decomposition processes observed must therefore occur either from the triplet state or from the singlet ground state.

The simplest scenario, in which the absorption process is followed by internal conversion to the ground state from which Me_4Si decomposes, does not explain the experimental results. If channel (I) has an activation energy as large as suggested above, it will be unable to compete with channel (II), the A factor of $k(I)$ being smaller and the activation energy being larger than the corresponding values of $k(II)$. Furthermore, unimolecular theory suggests that an Me_4Si molecule, with an internal energy equal to the photon energy, decomposes slowly enough to make the overall quantum yield pressure dependent. In the RRKM calculations for channel (II), a Gorin-type transition state was used, the
position of which has been determined variationally. With this transition state structure, we calculate a high-pressure A factor in agreement with experiment [45]. We obtain the microcanonical rate constant $k(E, \langle J \rangle) = 3 \times 10^7$ s^{-1} where $\langle J \rangle$ stands for the mean rotational quantum number at 300 K. The value for $k(E, \langle J \rangle)$ suggests that, especially in our experiments with SF_6, a substantial decrease in the overall quantum yield should be observed contrary to the experimental results.

The following experimental results give some indication as to the path taken by the excited molecule. Approximately one-third of the excited molecules will be deactivated under our experimental conditions. The kinetic behaviour of Me_2SiCH_2 formed in channel (I) agrees in every way with its electronic ground state formed by the disproportionation reaction of two Me_3Si radicals [19]. We therefore believe that Me_2SiCH_2 is formed in its ground state. Embedding the excited

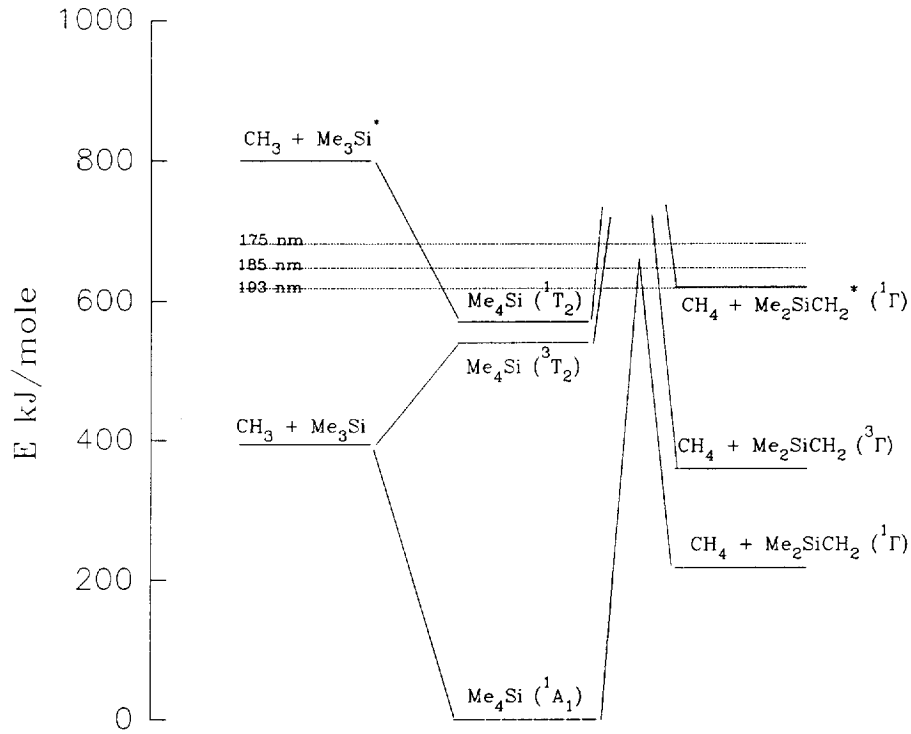

Fig. 21. Energy correlation diagram of the three lowest electronic states of Me_4Si and of various dissociation channels.

molecule in a liquid leads to a nearly complete elimination of channel (II), while the quantum yield of CH_4 formation remains unaffected [3]. This result seems to suggest that a dissociative state is involved in the formation of CH_4 and Me_2SiCH_2.

The last two seemingly contradictory results can be reconciled if we assume a curve crossing between the excited singlet state and the activation barrier for process (I) of the ground state potential energy surface. The Franck–Condon region reached by the absorption process is left by an E vibration towards a lower D_{2d} symmetry. On its way to the Jahn–Teller relaxed state, a transition to the ground state surface leads to a spontaneous dissociation into CH_4 and Me_2SiCH_2. The Franck–Condon region can also be left by a T vibration towards a C_{3v} state. Intersystem crossing to the close lying triplet state results in spontaneous Si–C splitting. In the liquid phase there are two possibilities: either intersystem crossing dies out and internal conversion to the ground state takes place or some molecules still decompose via the triplet state but re-form the reactant in the solvent cage (we thank a referee for constructive comments on this point). The strong interaction of the stable excited singlet state with the continuum states of the triplet and singlet ground state explains the structureless shape of the absorption band.

Acknowledgements

We thank C. Kerst, N. Arthur, J.E. Hudson and F. Mark for their help at different stages of this work.

References

[1] L. Gammie, C. Sandorfy and O.P. Strausz, *J. Phys. Chem., 83* (1979) 3075.
[2] S.K. Tokach and R.D. Koob, *J. Phys. Chem., 83* (1979) 774.
[3] E. Bastian, P. Potzinger, A. Ritter, H.P. Schuchmann, C. von Sonntag and G. Weddle, *Ber. Bunsenges. Phys. Chem., 84* (1980) 56.
[4] R.M. Martin and J.E. Willard, *J. Chem. Phys., 40* (1964) 2999.
[5] L.C. Glasgow and P. Potzinger, *J. Phys. Chem., 76* (1972) 138.
[6] Y. Harada, J.N. Murrell and H.H. Sheena, *Chem. Phys. Lett., 1* (1968) 595.
[7] R. Roberge, C. Sandorfy, J.J. Mathews and O.P. Strausz, *J. Chem. Phys., 69* (1978) 5105.
[8] M. Ahmed and P. Potzinger, unpublished results, 1992.
[9] J.A. Seetula, I.J. Russell and D. Gutman, *J. Am. Chem. Soc., 112* (1990) 1374.
[10] H.E. O'Neal, M.A. Ring, W.H. Richardson and G.F. Licciardi, *Organometallics, 8* (1989) 1968.
[11] W.V. Steele, *J. Chem. Thermodyn., 15* (1983) 595.
[12] T. Brix, N.L. Arthur and P. Potzinger, *J. Phys. Chem., 93* (1988) 8193.
[13] L. Gammie, I. Safarik, O.P. Strausz, R. Roberge and C. Sandorfy, *J. Am. Chem. Soc., 102* (1980) 378.
[14] S.K. Tokach and R.D. Koob, *J. Am. Chem. Soc., 102* (1980) 376.
[15] B.J. Conett, K.Y. Choo and P.P. Gaspar, *J. Am. Chem. Soc., 102* (1980) 377.

[16] D.J. Doyle, S.K. Tokach, M.S. Gordon and R.D. Koob, *J. Phys. Chem., 86* (1982) 3626.
[17] T. Brix, E. Bastian and P. Potzinger, *J. Photochem. Photobiol. A: Chem., 49* (1988) 287.
[18] I. Safarik, A. Jodhan, O.P. Strausz and T.N. Bell, *Chem. Phys. Lett., 142* (1987) 115.
[19] C. Kerst, *Ph.D. Thesis,* Göttingen, 1994.
C. Kerst, P. Potzinger and H. Gg. Wagner, publication in preparation.
[20] S.K. Tokach and R.D. Koob, *J. Phys. Chem., 84* (1980) 1.
[21] T.N. Bell, A.G. Sherwood and G. Soto-Garrido, *J. Phys. Chem., 90* (1986) 1184.
[22] A.H. Laufer, *Rev. Chem. Intermed., 4* (1981) 225.
[23] J.N. Bradley, H.W. Melville and J.C. Robb, *Proc. R. Soc. London, Ser. A, 236* (1956) 318.
A.H. Turner and R.J. Cvetanovic, *Can. J. Chem., 37* (1959) 1075.
[24] R. Walsh, in S. Patai and Z. Rappoport (ed.), *The Chemistry of Organic Silicon Compounds,* Wiley, 1989.
[25] D.F. McMillen and D.M. Golden, *Annu. Rev. Phys. Chem., 33* (1982) 493.
[26] I.M.T. Davidson, P. Potzinger and B. Reimann, *Ber. Bunsenges. Phys. Chem., 86* (1982) 13.
[27] M.C. Flowers and L.E. Guselnikov, *J. Chem. Soc. B,* (1968) 419.
[28] P. John, B.G. Gowenlock and P. Groome, *J. Chem. Soc., Chem. Commun.,* (1981) 806.
[29] S. Satyapal, J. Park and R. Behrson, *J. Chem. Phys., 91* (1989) 6873.
[30] J.T. Jodkowski, E. Ratajczak, A. Silesen and P. Pagsberg, *Chem. Phys. Lett., 203* (1993) 490.
[31] L.N. Krasnoperov, J. Niiranen and D. Gutman, *12th Int. Symp. Gas Kinetics, Reading, 1992.*
[32] I.M.T. Davidson and C.E. Dean, *Organometallics, 6* (1987) 966.
[33] S. Sakai and M.S. Gordon, *Chem. Phys. Lett., 123* (1986) 405.
[34] N. Shimo, N. Nakashima and K. Yoshihara, *Chem. Phys. Lett., 125* (1986) 303.
[35] T. Turanyi, *Comput. Chem., 14* (1990) 253.
[36] W. Tsang, *Combust. Flame, 78* (1989) 71.
[37] M.B. Robin, *Higher Excited States of Polyatomic Molecules,* Academic Press, 1985.
[38] S. Evans, J.C. Green, P.J. Joachim, A.F. Orchard, D.W. Turner and J.P. Maier, *J. Chem. Soc., Faraday Trans. II, 68* (1972) 905.
[39] A.E. Jones, G.K. Schweitzer, F.A. Grimm and T.A. Carlson, *J. Electron Spectrosc., 1* (1972) 29.
[40] L. Szepes and T. Baer, *J. Am. Chem. Soc., 106* (1984) 273.
[41] H. Hirayama and J. Lipsky, *J. Chem. Phys., 51* (1969) 3616.
[42] L. Ding and P. Marshall, *J. Am. Chem. Soc., 114* (1992) 5754.
[43] E.V. Sokolova, T.F. Danilova, G.N. Shvets, L.E. Guselnikov, V.V. Volkova, V.A. Klyuchnikov and M.G. Voronkov, *Metalloorg. Khim., 6* (1991) 97.
[44] J.A. Boatz and M.S. Gordon, *J. Phys. Chem., 95* (1991) 7244.
[45] A.C. Baldwin, I.M.T. Davidson and M.D. Reed, *J. Chem. Soc., Faraday Trans. I, 74* (1978) 2171.
[46] W.L. Hase and J.W. Simons, *J. Chem. Phys., 52* (1970) 4004.
[47] M.S. Gordon and T.N. Truong, *Chem. Phys. Lett., 142* (1987) 110.
[48] S. Wolfe and C.K. Kim, *Israel J. Chem., 33* (1993) 295.
[49] G. Raabe and J. Michel, *Chem. Rev., 85* (1985) 419.